ELSEVIER

Journal of Structural Geology 25 (2003) 2053–2076

JOURNAL OF STRUCTURAL GEOLOGY

www.elsevier.com/locate/jsg

Tectonics of the Akamas and Mamonia ophiolites, Western Cyprus: magnetic petrofabrics and paleomagnetism

G.J. Borradaile*, K. Lucas

Geology Department, Lakehead University, Thunder Bay, ON, Canada P7B 5E1

Received 5 July 2002; received in revised form 14 January 2003; accepted 17 February 2003

Abstract

The Akamas ophiolite is shown to be a distal, off-axis extension of the main outcrop of Cretaceous ophiolite in the Troodos complex of Cyprus. Mantle-sequence harzburgites of both ophiolites share similarly oriented mantle-flow fabrics and the same Tertiary magnetizations acquired during exhumation. However, compared with the Troodos mantle sequence rocks, the Akamas ferromagnetic mineralogy is more oxidized and remanences with lower blocking temperatures were acquired chemically. Paleopoles calculated from published vectors and our own new data define an apparent polar wander path (APWP) for the Troodos microplate. The APWP shows that between 88 and ~50 Ma the Troodos microplate was equatorial and the vertical axis for its 60° anticlockwise rotation was located within the microplate. Subsequently, the microplate drifted northward to 34°N with minor anticlockwise rotation at a reduced rate. That requires microplate-rotation about a vertical axis located to the west of Cyprus in the last ~50 Ma. The allochthonous Triassic Mamonia terrane docked with the Cretaceous Troodos terrane in SW Cyprus. Within it, disrupted tectonized ophiolite has been regarded as part of a Triassic ocean floor or as sheared fragments of Cretaceous Troodos ophiolite, incorporated into the Mamonia terrane when it docked with the Troodos terrane. Whatever their provenance, their paleomagnetic signals postdate their penetrative deformation and metamorphism and their paleopoles may still be used to track their post-strain motion. Our calculations of paleopoles from published vectors for the Mamonia terrane smear along an extension of the APWP for the Troodos microplate that is, moreover, concentric with the Troodos microplate. This suggests that the paleopole dispersion of the Triassic Mamonia rocks and their post-magnetization disruption occurred during their accretion onto the anticlockwise-spinning Troodos microplate.

Keywords: Cyprus; Ophiolite; Magnetic fabrics; Plate tectonics; Apparent polar wander path

1. Introduction

Cyprus provides access to the best understood and first documented ophiolite sequence on dry land (Gass, 1968; Vine and Moores, 1969). Its significance was appreciated early, just as contemporary ideas of ocean-floor spreading received widespread acceptance (Vine and Matthews, 1963; Vine, 1966). This classic ophiolite sequence has strongly influenced formulation of the plate tectonic paradigm (Gass, 1968; Moores and Vine, 1971; Clube et al., 1985; Varga and Moores, 1985; Malpas et al., 1990; Gass et al., 1994). Located in the eastern Mediterranean, the Troodos massif of Cyprus is a window into the remains of the nearly closed Tethys ocean, revealing an uplifted, complete ophiolite sequence (Fig. 1). The latter is complete from pelagic sediments, down through the now universally recognised ophiolite 'stratigraphy' of pillowed basalt, sheeted-dikes and mantle-sequence mafic rocks, in descending order. Fortunately, this ophiolite happens to be of the simplest type in the Eastern Mediterranean, in terms of magmatic stratigraphy and internal structure (Whitechurch et al., 1986). This lead to the early association of ophiolites with the ocean-floor spreading mechanism (Gass, 1968; Moores and Vine, 1971) and also to the success of paleomagnetism in recognising the independent, Troodos-microplate (Vine and Matthews, 1969; Moores and Vine, 1971; Clube et al., 1985; Allerton and Vine, 1987; Hurst et al., 1992).

Although they have received comparatively little attention, there are two other, tectonically distinct ophiolite exposures in Cyprus, whose ages and relationships to the Troodos ophiolite are unclear. These are the focus of attention in this paper (Fig. 1). One crops out in the Akamas

* Corresponding author. Tel.: +1-807-343-8461; fax: +1-807-935-2753.
E-mail address: borradaile@lakeheadu.ca (G.J. Borradaile).

0191-8141/03/$ - see front matter © 2003 Elsevier Ltd. All rights reserved.
doi:10.1016/S0191-8141(03)00046-4

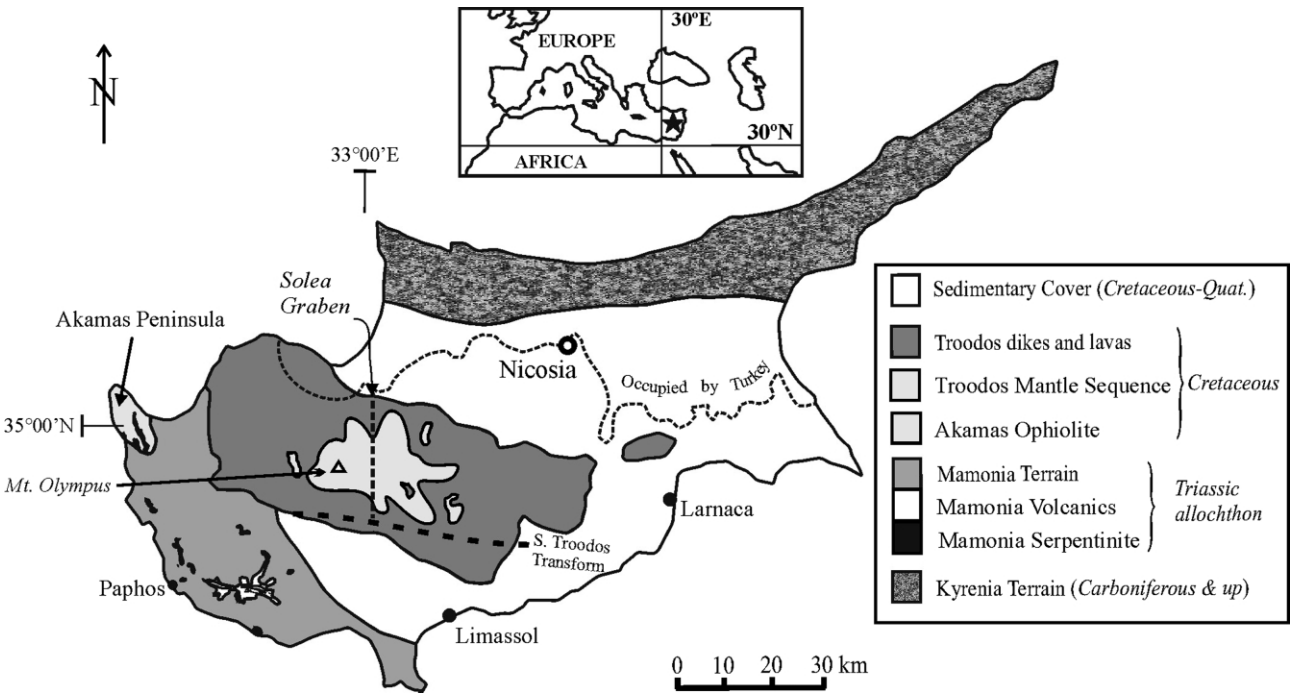

Fig. 1. Location of Cyprus and the main tectonic units comprising the island. This paper is concerned with the paleomagnetic and tectonic relationships among the Troodos, Akamas and Mamonia ophiolites, using new data for Akamas and Troodos, integrated with calculations of paleopoles from previous published paleomagnetic vectors.

peninsula, having about 20% of the surface area of the well-known Troodos complex. The other is represented by scattered exposures of disrupted ophiolites within the Mamonia terrane of SW Cyprus. The Mamonia terrane sedimentary rocks have a Triassic fauna (Henson et al., 1949; Ealy and Knox, 1975), corroborated by geochronology (LaPierre and Rocci, 1969). However, the provenance of the Triassic sedimentary rocks is unclear and that of the included ophiolite slivers is more problematic. They have been correlated with rocks that occur in the Kyrenia terrane of N. Cyprus and in the Antalaya Group of Turkey (Robertson and Woodcock, 1979) but they have also been attributed to a southern provenance (Ealy and Knox, 1975). Although the balance of the literature tips in favour of a correlation of the Akamas ophiolite with Troodos, the relationships amongst the Akamas, Troodos and Mamonia ophiolites have not been addressed directly. Against this fairly complicated background of research, the next two sections review some relevant elements of Cyprus geology.

2. The three basement terranes: Kyrenia, Troodos and Mamonia

The Troodos massif forms one of three foundation tectonic units of Cyprus, sandwiched between the older Kyrenia terrane to the north and the Mamonia terrane to the south (Fig. 1). Attention has logically focused on the main ophiolite outcrop of the Troodos Massif, a mountainous region exposing the core of a dome, in the centre of which the deepest mantle-sequence rocks are found (Fig. 1). Its study advanced understanding of the structure, tectonics and paleomagnetism of ocean-floor spreading. In this respect, the Troodos massif is particularly valuable as it exposes three spreading-axes (Varga and Moores, 1985; MacLeod et al., 1990; Moores et al., 1990; Varga et al., 1999), the earliest and most easterly being the Solea Graben (Fig. 1), and a fossil transform fault along the south flank of the Troodos massif (e.g. Moores and Vine, 1971; Gass et al., 1994). Penetrative secondary tectonic deformation, in the sense of traditional structural geology, is absent, but in the region of faults, particularly within 10 km of the southern Troodos Transform Fault Zone, cataclasis is extensive and dike-trends are sheared (e.g. Gass et al., 1994; also see Bonhommet et al., 1988). The only true penetrative petrofabrics, yielding preferred orientation-distributions, are found as early or primary plutonic-flow fabrics in harzburgite and lherzolite of the upper mantle sequence (Borradaile and Lagroix, 2001). The cataclastic modification of the penetrative mineral-alignment fabrics appears to be a relatively early event associated with high temperature flow and subsequent serpentinization. The Troodos ophiolite is accepted as late Cretaceous oceanic crust and mantle, created between approximately 88 and 75 Ma. The Troodos microplate formed above a northwards-descending subduction zone, but rotated rigidly about a vertical axis with a clockwise sense through ~90° in the interval from 92 to 88 Ma (Moores and Vine, 1971; Clube et al., 1985; Clube and Robertson, 1986). Our paleopole determinations verify the earlier implicit assumption that

the rotation-axis was located within the Troodos microplate. The Tertiary sedimentary cover to the Troodos terrane also blankets the adjacent Triassic Mamonia terrane that was sutured onto the Troodos microplate, dating their amalgamation at ≤65 Ma (Fig. 2) (Clube and Robertson, 1986).

A second, significant large exposure of harzburgite crops out on the Akamas peninsula of western Cyprus, with discontinuous outcrops of related higher level ophiolite along the shores of the peninsula (Fig. 2). The ophiolites of the northern Akamas peninsula are regarded as an outlier of Troodos microplate ophiolite together with some disjunctive exposures in SW Cyprus, within the Mamonia terrane (Clube and Robertson, 1986; Robertson, 1990; Bailey et al., 2000). The Mamonia sedimentary rocks contain Triassic fauna, of Karnian–Norian age (230–210 Ma) and volcanic material of ~210 Ma (LaPierre and Rocci, 1969) and by inference some of the ophiolite inliers have been regarded as integral components of the Mamonia terrane, fragments of the earlier Triassic ocean floor (Henson et al., 1949; Ealy and Knox, 1975; Morris et al., 1998). However, some are mapped as Troodos age ophiolite by Bailey et al. (2000). The Mamonia ophiolites of SW Cyprus have thus been

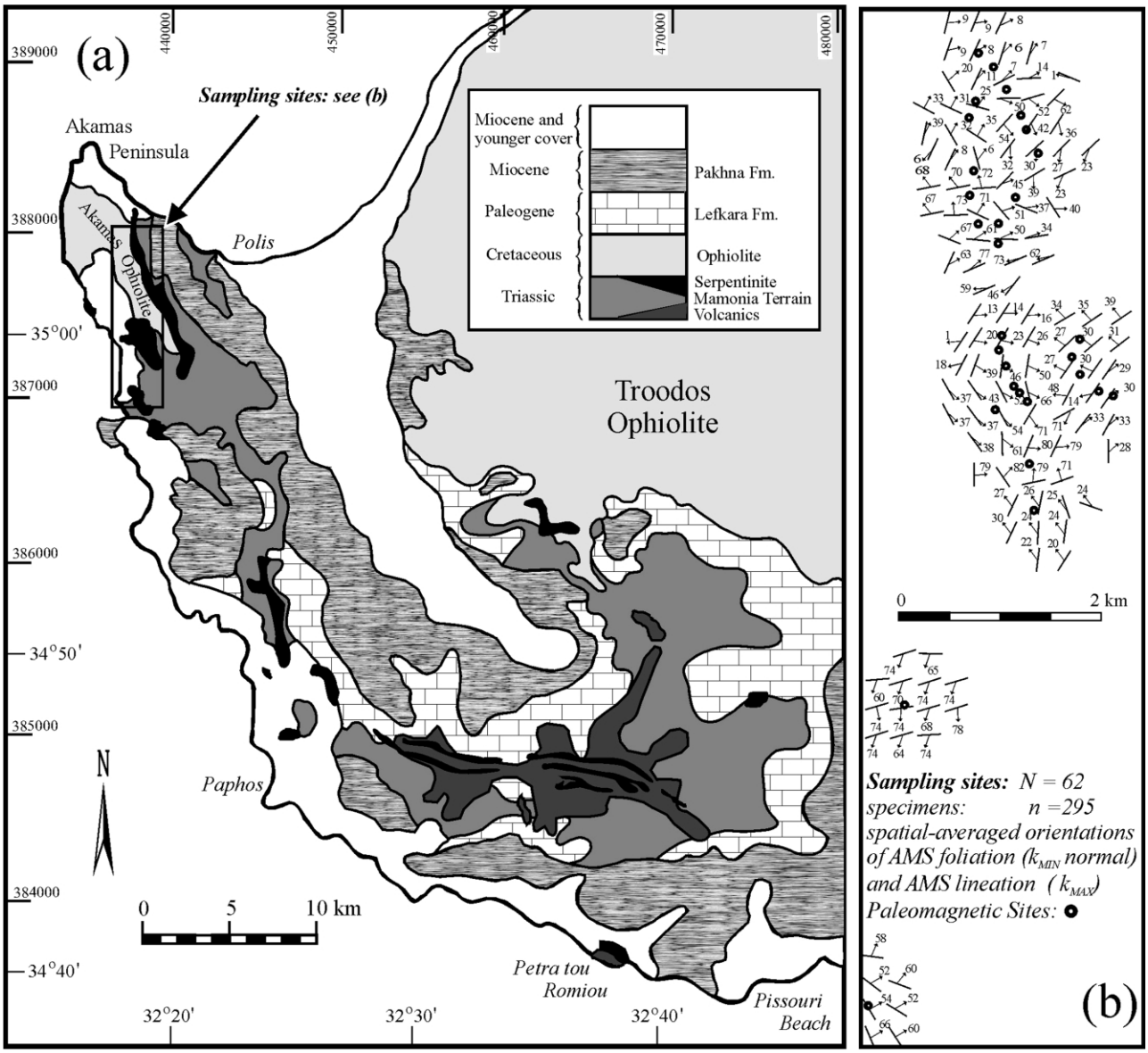

Fig. 2. (a) Simplified geology of SW Cyprus, after the Geological Survey Department of Cyprus. The Mamonia terrane is a Triassic sequence, including ophiolite, sutured to the Cretaceous microplate in the Miocene. Paleontology and geochronology constrain formation-ages for the Troodos massif. However, the Mamonia sequence is a tectonically disrupted allochthonous sequence of ophiolite, sedimentary, volcanic and metamorphic rocks with a limited Karnic–Norian Triassic fauna (Henson et al., 1949), confirmed geochronologically (215 ± 10 Ma) at one site, Petra tou Romiou (LaPierre and Rocci, 1969). (b) Distributions of sites at which magnetic fabrics were studied in the Akamas peninsula. Tensor-mean orientations of the AMS ellipsoid that defines a magnetic foliation ($k_{MAX} - k_{INT}$ plane) and a magnetic lineation (k_{MAX}) are spatially averaged. Spatial averaging used a 250 m diameter counting circle, weighting the orientations inversely with distance from the counting station.

regarded as Triassic (pre-210 Ma) or as Cretaceous ophiolite of Troodos, incorporated within the Mamonia terrane by faulting during its collision with the Troodos microplate. Whatever their affinity, their post-penetrative deformation paleomagnetism reveals their post-metamorphic movements on the Tethyan ocean-floor.

The Akamas are more intensely fractured, sheared and weathered than those of Troodos and outcrop relationships more obscure. The Akamas exposure is occupied by mantle sequence rocks, mostly medium-grained to coarse-grained harzburgite that are accepted as a distal extension of the Troodos complex (e.g. Bailey et al., 2000). We will show that their preferred mineral orientations are similarly oriented to those in the Troodos massif. Moreover, our new paleomagnetic information and the calculation of paleopoles from previously published vectors will demonstrate the terrane motion for the Troodos and Mamonia terranes.

The Kyrenia terrane presents the steepest, most rugged topography on the island. Its tectonic deformation is severe with some tight folding on E–W axes and southwards upthrusting due to Eocene, N–S compression (Clube and Robertson, 1986). The post-tectonic Quaternary sediments of the Mesaoria plain obscure contacts between the Kyrenia terrane and the Troodos ophiolite. However, their tectonic contact is inferred at depth (Robertson and Xenophontos, 1993). The Kyrenia terrane exposes deformed sedimentary rocks of Permian (and perhaps Carboniferous) to Eocene age, comparable with the Antalaya Complex of Southern Turkey (Clube and Robertson, 1986). This is pertinent to our discussion because it includes correlatives of the Triassic Mamonia sequence and may imply a northern provenance for some Mamonia terrane sedimentary rocks.

3. Relationship of Troodos Microplate to the Mamonia allochthon

Cyprus comprises four main geological terranes (Fig. 1). The Cretaceous–Quaternary cover represents a shallowing upward sequence of sediments. Its regional structure is simple, with strata dipping gently away from the Mt. Troodos, usually at $<10^{\circ}$. This is due to the exhumation of the Troodos complex. Regional depressions and culminations with gentle dips ($<10^{\circ}$) are superimposed on this simple pattern due to local flexures and primary depositional basins (Lagroix and Borradaile, 2000). Only rarely are any penetrative structural elements or steep dips found, usually associated with localized fault formation, e.g. in the Yeresa belt, south of Limassol Forest. The simple, gentle tilting and absence of penetrative deformation render the interpretation of paleomagnetic data particularly easy and confident. A similar degree of structural simplicity is shown by the Troodos complex itself. Paleopoles are calculated without tilt-corrections that require complex and stringent assumptions (MacDonald, 1980; Borradaile, 1997, 2001a,b) that may degrade the results. This is validated by the great consistency of the paleopole distribution (Fig. 10). The sedimentary cover sutures the three basement terranes, Kyrenia, Troodos and Mamonia as a single unit during subsequent microplate rotations. The Mamonia terrane is much more deformed and provides the only consistently penetratively strained formations in Cyprus, including regionally metamorphosed rocks. Thus, paleopoles for the Mamonia terrane record terrane-rotation that postdates the structural complexities recorded by folding, cleavage and thrusting seen in some outcrops.

The island's early tectonic history follows from an analysis of the relationships between the Kyrenia sedimentary sequence of northern Cyprus, perhaps as old as Carboniferous; the Cretaceous ocean-floor sequence of Troodos; and the mostly Triassic sedimentary, metamorphic and volcanic Mamonia allochthon of SW Cyprus. We will attempt to refine the relationships between the Mamonia and Troodos terranes, in particular focusing on their intimate and sometimes unclear relationships in the Akamas peninsula. Our approach includes the use of magnetic petrofabrics and paleomagnetism. Magnetic fabrics provide a remarkably clear picture of the penetrative mineral alignments that are obscured in the field due to weathering and less significant, secondary cataclasis. Paleomagnetic records define paleopole positions and thus microplate-rotations since the remanences were acquired, post-cataclasis.

The uplifted Cretaceous (Turonian) Troodos ophiolite, a fragment of Neo-Tethyan ocean-floor that includes a complete profile from mantle-sequence harzburgites, through sheeted dikes, pillowed basalts to pelagic chalk cover (e.g. Robertson and Woodcock, 1979). The ocean-floor structure is revealed clearly on land with several spreading axes now reoriented N–S, and a major transform fault zone along the southern edge of Troodos, now oriented E–W (e.g. Moores and Vine, 1971; Malpas et al., 1990; Gass et al., 1994). The Troodos ophiolite shows a classic ocean-floor 'stratigraphy' but geochemically it is depleted in rare-earth elements with respect to typical Mid-Ocean Ridge basalts. This prompted Malpas et al. (1993, their fig. 8) to propose the ophiolite formed above a subduction zone, fed by already depleted magma. Subduction was shown to have been from the south. The dispersion of paleomagnetic inclinations shows the Troodos ophiolite rotated $>90^{\circ}$ anticlockwise since the Turonian (e.g. Clube and Robertson, 1986). However, comparisons with other ophiolites now suggest that the underlying mantle may have been depleted elsewhere, its chemical signature reflecting mantle-history rather than invoking a specialized supra-subduction setting for the Troodos complex (Moores et al., 2000). In either case, the microplate rotations are unaffected by petrogenetic interpretation.

The Mamonia sedimentary, metamorphic and volcanic rocks are also found in SW Cyprus, where their Triassic biostratigraphic age (Henson et al., 1949) was confirmed radiometrically at $\sim 215 \pm 10$ Ma (LaPierre and Rocci,

1969). They comprise volcanic rocks, ophiolite, and epidote-amphibolite metasedimentary rocks and are juxtaposed with ophiolite on the Akamas peninsula. They are thrust and recumbently folded up to the NE and sinistrally sheared along steep serpentinized fault-zones (Robertson and Woodcock, 1979). Their location south of the Cretaceous Troodos ophiolite but north of the inferred subduction zone was difficult to interpret (e.g. Ealy and Knox, 1975). Some workers considered parts of the Akamas ophiolite, with geochemical affinities to Troodos (Swarbrick, 1993), as a distal extension of the main Troodos ophiolite outcrop of Central Cyprus, separated only by the Pliocene-filled, Polis rift valley (e.g. Clube and Robertson, 1986). Others consider all or part of the Akamas ophiolites to be extensions of the Mamonia ophiolites of SW Cyprus (e.g. Robertson and Xenophontos, 1993; cf. Robertson and Woodcock, 1979; Morris et al., 1998). Well within identifiable Mamonia terrane of SW Cyprus, volcanic rocks and serpentinized ophiolite mingle tectonically with Triassic sediment that are widely regarded as fragments of Triassic ocean-floor, with a more typical ocean-floor basalt signature, whereas the Troodos ophiolite's geochemistry differs due to some depletion mechanism, but not necessarily requiring a supra-subduction setting as discussed above. The tectonic juxtaposition of Cretaceous and Triassic ocean-floor (the latter of more typical MORB geochemistry) invites speculation about the absence of Jurassic ocean-floor. Whereas complete subduction is an attractive and logical possibility, we show that there is little paleomagnetic evidence for the required latitudinal translation. Moreover, on tectonic grounds there may have been little space to accommodate much Jurassic ocean-floor (Robertson and Woodcock, 1979). Microplate rotation provides the most viable tectonic explanation (Clube and Robertson, 1986, their fig. 15), implicitly about a local vertical axis. However, we will show that rotation about a distant axis is also required (Fig. 12).

4. Magnetic fabrics

Our first step toward understanding the relationships among the three ophiolites was to compare their petrofabrics. Simplistically, if similar primary ophiolite-flow fabric orientations are found, any correlation is strengthened. The tectonized, serpentinized and disrupted ophiolites and volcanic rocks of the Mamonia terrane are not suitable. Their fabrics are clearly secondary and entirely tectonic. However, the similarity of the Akamas and Troodos ophiolites has been noted by others. Logically, a correlation of the fabrics in their deepest units, the mantle-sequence harzburgites, might illustrate some similar mantle-flow regime that could validate the correlation.

The orientation-distribution of mineral grains has always been a useful clue to the kinematic history of rocks, using outcrop-observations to infer major tectonic movement patterns. However, in many rocks, petrofabric orientations and intensities are difficult to detect in the field and are only poorly defined after considerable laboratory processing of petrographic information. For several reasons, magnetic anisotropy has become a popular tool to detect preferred mineral orientations (Hrouda, 1982; Borradaile and Henry, 1997). If induced magnetization is recorded, in the presence of an applied field similar to the Earth's field in strength ($\sim$0.1 mT), the anisotropy is referred to as anisotropy of magnetic susceptibility (AMS). This is susceptibility to induced magnetization in low field, which disappears when the field is removed. No permanent magnetization is involved and any natural remanent magnetization (NRM) is left undisturbed by this procedure. The low field is applied to a cylindrical sample, 25 mm in diameter by 22 mm high along various specimen-axes for which magnetic susceptibility is measured. Cores were prepared under a tilting-vice laboratory drill-press, from oriented field-specimens. From each specimen at least three cores were prepared. AMS was determined for every core and at least one core per specimen was reserved for AARM determination (see below), which destroys the NRM. At least two cores from each specimen, were reserved for paleomagnetic studies without the exposure to high fields such as used during AARM determination.

For each specimen, we determined AMS from susceptibility measurements along seven different axes through the specimens. The combination of body-diagonal and edge-parallel measurements with respect to specimen coordinates considerably improves precision (Borradaile and Stupavsky, 1995). Susceptibility was measured in a Sapphire Instruments SI2B device operating at 19,200 Hz and $\sim$0.1 mT with the interactive data acquisition and processing software package SI201.exe. From measurements along six or more suitably chosen axes, the second rank tensor describing anisotropy of susceptibility was determined. Where the magnitudes of all axes have the same sign, the second rank tensor is conveniently envisaged as an ellipsoid. Structural geologists sometimes loosely compare this to a strain-ellipsoid although, at best, the AMS ellipsoid only represents the orientation-distribution of the combination of minerals that dominate the magnetic susceptibility (Borradaile, 1991; Borradaile and Henry, 1997). The fabric ellipsoid or orientation-distribution matrix of petrofabrics (Flinn, 1965; Woodcock, 1977) is usually a more accurate analogy for the AMS ellipsoid.

The AMS of rock specimens integrates contributions from several sources. The matrix-forming minerals are usually of greatest interest in structural geology and their AMS is crystallographically controlled. However, since most rock-forming silicates have monoclinic or lower symmetry, there cannot be a very strong correspondence of crystallographic axes with AMS axes (Nye, 1957; Borradaile and Werner, 1994; Lagroix and Borradaile, 2000). Moreover, many matrix forming minerals, especially mafic silicates, contain inclusions of high-susceptibility

accessory minerals. The most important accessory mineral in this context is magnetite. Due to its high susceptibility, its AMS is controlled by grain-shape, whether it is an inclusion or an independent accessory grain. The degree to which AMS reflects different aspects of the orientation distribution of silicates, magnetite inclusions and free magnetite accessories require careful assessment by statistical and experimental methods, discussed next.

Accessory minerals of unusually high susceptibility may have a different orientation-distribution related to crystallization in a later stress-field and compete with the contribution from the tectonically more interesting fabric of matrix-minerals. In our case, magnetite, ilmenite and titanomagnetite-series minerals produce a high-susceptibility subfabric that blends with the AMS signature due to the silicates' orientation-distribution. The confounding of the orientation-distribution contributions of high-susceptibility accessories and of the matrix minerals may be resolved by three data-processing approaches (i–iii) and by two experimental techniques (iv and v).

(i) Although it is rarely possible and generally unreliable, one may attempt to subtract mathematically the contribution of the high-susceptibility accessory minerals from AMS.
(ii) The frequency distribution of susceptibility-magnitudes may be different for specimens with different AMS orientations or anisotropy-degree, permitting one to isolate separate subfabrics (Borradaile and Gauthier, 2001). If the orientation-distributions are recognisable as separate modes on a stereogram, it may be possible to isolate and subtract one or more directly. Of course, the orientations must be carefully associated with the magnitudes that they represent for this procedure to be valid.
(iii) One may reduce the influence of the orientation distribution of minerals of anomalously high susceptibility by standardizing all specimens to the same unit-value susceptibility. This is demonstrated below by illustrating the mean tensor for standardized and non-standardized specimen-tensors.
(iv) Experimentally, one may isolate the AMS contribution of paramagnetic minerals such as the matrix-forming silicates. Their magnetization response to applied fields is linear and they do not show saturation, like the remanence-bearing 'ferro'magnetic minerals such as magnetite. Thus, the determination of anisotropy in very high fields can suppress the contribution from non-paramagnetic sources (Stacey and Banerjee, 1967; Jelinek, 1985; Parma, 1988). The procedure is time-consuming and destroys the specimens' NRM that may be required for paleomagnetic purposes.
(v) Alternatively, as in this study, one may experimentally isolate the anisotropy of the remanence-bearing minerals, in this case principally magnetite and titanomagnetite. The most secure technique is to determine the anisotropy of anhysteretic remanence (AARM) (McCabe et al., 1985; Stephenson et al., 1986; Jackson, 1991). However, with care, a simpler procedure is to determine the anisotropy of isothermal remanence (Daly and Zinsser, 1973; Borradaile and Dehls, 1993; Jelinek, 1996). These procedures, especially AARM, are more time-consuming than AMS, requiring at least 20 min per specimen as opposed to approximately 3 min for the determination of AMS. AMS should always be determined before AARM as exposure to high fields may change the AMS due to domain-wall rearrangements in remanence-bearing phases (Potter and Stephenson, 1990; Stephenson and Potter, 1996). Anisotropy of remanence merges the contributions of the orientation-distributions of all the remanence-bearing minerals, e.g. magnetite, titanomagnetite, pyrrhotite, hematite but the shape-controlled AMS of magnetite usually predominates due to its very high bulk susceptibility. However, the fabric-contribution of ilmenite is not isolated by room-temperature remanence-anisotropy experiments since it only retains a remanence below −218 °C.

4.1. AMS: anisotropy of magnetic susceptibility

Oriented hand-specimens were retrieved from 65 outcrops and drilled in geographic coordinates to yield 293 cores (25 mm in diameter and 22 mm high). For the purposes of structural interpretation and comparison with more elusive field structures (Bailey et al., 2000), the AMS ellipsoid may be reduced to a magnetic foliation (k_{MAX} − k_{INT} plane) and a magnetic lineation (k_{MAX}) that represent the dominant orientation-distribution of minerals. The orientations have been tensor-averaged and spatially-averaged at each site, using 250 m counting circles. Data are weighted in inverse proportion to their distance from the counting station and illustrate a consistent smooth variation in petrofabric orientations across the Akamas mantle sequence rocks (Fig. 2b). Despite the fractured appearance of the rocks in the field, the petrofabric appears satisfactorily homogeneous, with simple unimodal distributions revealed by the contoured density plots of individual susceptibility axes (inset left, Fig. 3). Although the Akamas mantle-sequence rocks show a composite cataclastic and penetrative, E-dipping foliation in many outcrops their intrinsic petrofabric orientations (Fig. 3) are very similar to those of the Troodos massif, around Mount Olympus, shown in Fig. 5 (Borradaile and Lagroix, 2001). Given the simple, spatial variation in orientation of petrofabrics across the Akamas peninsula (Fig. 2b) and unimodal orientation-distributions (Fig. 3), it is meaningful to proceed with analysis using tensor-statistics (Jelinek, 1977, 1978) that may be differently applied, depending on the interpretive goal (Borradaile, 2001a, 2003).

Averaging the orientations of individual specimen tensors for AMS is a complex procedure because both the

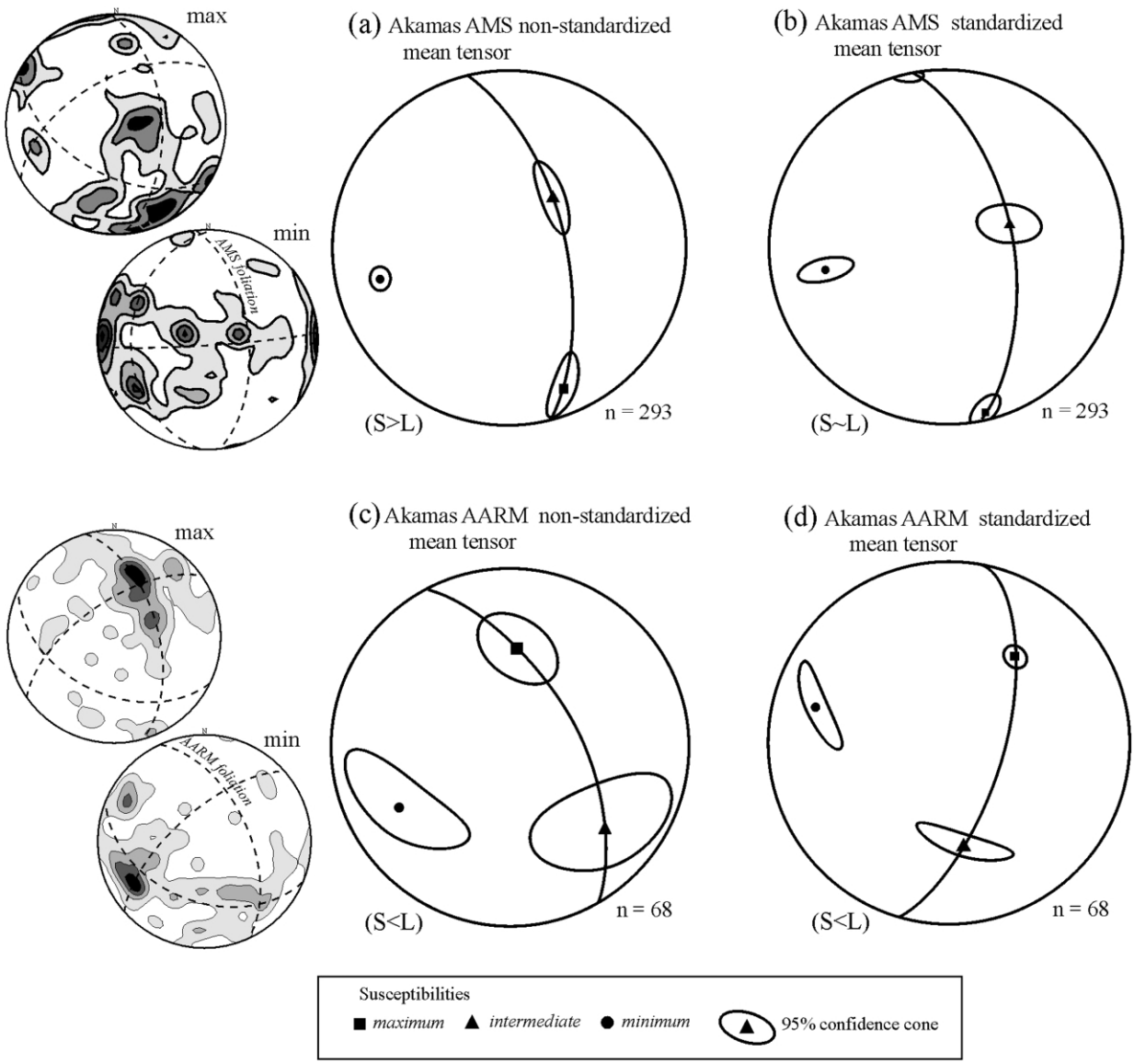

Fig. 3. Magnetic fabrics reveal the orientation-distribution of minerals, aligned by tectonic flow in these harzburgites from Akamas. Density contours of k_{MAX} and k_{MIN} axes for individual specimens inset (left) are contoured in multiples of the expected uniform density. The shape of the *orientation-distribution ellipsoid*, in the sense of Woodcock (1977) is designated using the L, S terminology of Flinn (1965). (a, b) Anisotropy of magnetic susceptibility (AMS) reveals the preferred orientation of paramagnetic mafic silicate, contaminated with aligned magnetite inclusions, and accessory free magnetite. Where the two differently responding mineral groups have sufficiently different bulk-susceptibilities they may be distinguished by comparing the orientations of their standardized and non-standardized mean-tensors (Borradaile, 2001a). For AMS, the mean-tensor of standardized specimens suppresses the role of mineral phases with anomalous orientations or anomalously high bulk-susceptibilities. (c, d) Anisotropy of anhysteretic remanence isolates the orientation-distribution of accessory magnetite in these rocks. The standardized version of the mean-tensor reduces the contribution of spuriously-oriented, high-susceptibility outliers.

magnitudes of the specimen-tensor's axes and their variation in orientation affect the orientation of the mean-tensor. Moreover, the axes of the mean tensor must be orthogonal, just like those of the individual specimen tensors. Although the magnitudes of the specimens' axes have little kinematic meaning or petrofabric value, they do affect the averaging process and differently oriented mean tensors may be determined if the magnitudes of the specimen-tensors are standardized to unit-value. This has considerable interpretive value since it provides a means of suppressing the role of subfabrics with anomalously high susceptibility, e.g. the subfabric of accessory magnetite. A further value of tensor-statistics is the provision of confidence limits around the mean tensor axes. Ideally and simply these should show orthorhombic symmetry with their shape dictating whether the orientation-distribution of minerals is an L-, L–S or S-fabric. However, the confidence cones may also be oblique to the principal symmetry planes of the mean-tensor, providing important clues as to the role of subfabrics with anomalous bulk susceptibility (Borradaile, 2001a).

The orientation of the mean-tensor for the AMS measurements is shown in Fig. 3a and b. AMS proxies as an integrated orientation-distribution for the preferred

crystallographic orientation of mafic silicates (Borradaile and Werner, 1994; Borradaile and Lagroix, 2001; Lagroix and Borradaile, 2001) and the preferred dimensional orientation of high susceptibility accessory minerals (Borradaile and Henry, 1997). Relative roles of their subfabrics in the mean-tensor are revealed by different statistical treatments (Jelinek, 1978; Borradaile, 2001a). Due to the enormous range of susceptibility values of minerals, over at least five orders of magnitude, the subfabric of accessory minerals with high susceptibility, in particular magnetite, ilmenite and titanomagnetite-series minerals, may contribute as much to whole-rock AMS as the silicate matrix. The AMS of the rock is sensitive to the balance between the anisotropy, bulk susceptibility and concentration of the high-susceptibility accessory minerals and of the matrix minerals, as well as the respective strengths of their orientation-distributions. This gives rise to competition between the orientation-distribution of high-susceptibility, weakly anisotropic phases like magnetite and that of the lower susceptibility, higher anisotropy silicates (Borradaile, 1987). Of the five possible approaches to the distinction of silicate and magnetite subfabrics that we listed above, we chose the following methods:

(ii) orientation distributions compared with mean susceptibility (Borradaile and Gauthier, 2001)
(iii) mean tensors compared for standardized and non-standardized specimens (Borradaile, 2001a)

and, in the following section;

(v) anisotropy of magnetite isolated by the AARM technique (Jackson, 1991).

The first statistical procedure, outlined above, allows us to evaluate the importance of high-susceptibility accessory phases in the rocks' AMS. It also permits the identification of inverse or blended fabrics, due to significant fractions of single-domain magnetite (Rochette et al., 1991, 1992, 1999) and has been useful in that context in Cyprus ophiolites (Borradaile and Gauthier, 2001). Perfect inverse fabrics due to single-domain magnetite are rare but there are many examples where its subordinate role is detectable in blended or 'intermediate' fabrics (Rochette et al., 1992). We found no evidence for such fabrics in these rocks, nor in the Troodos complex. The fabrics are of 'normal' type; k_{MAX} corresponds to mean alignment of mineral-elongation and k_{MIN} is normal to foliation.

The next statistical procedure is more revealing in this study; we compared mean-tensors for the entire sample, for the sample of specimens excluding statistical-outliers of high bulk susceptibility, and compared also the mean-tensors for the standardized and non-standardized specimen-tensors. The latter is most instructive; when the specimen tensors are directly averaged by tensor statistics, specimens of high bulk susceptibility may skew the orientation of the mean tensor. If we standardize all the specimen tensors by dividing them by their bulk value, they are all assigned equal weight and the anomalous orientation of any high-susceptibility outliers is subdued (Borradaile, 2001a). In effect, each specimen is reduced to unit-susceptibility. Although the orientations of anomalous specimens are still included in the mean tensor they have less or even negligible effect on the overall orientation-distribution. Therefore, the mean-tensor for standardized specimens more closely approximates the orientation-distribution of the matrix minerals. Large differences between the orientations of the mean tensors of standardized and non-standardized specimens indicate the presence of a non-coaxial subfabric. Such situations commonly arise where mineral subfabrics of different bulk-susceptibility crystallize at different stages in a non-coaxial strain history (Borradaile and Henry, 1997).

In the Akamas ophiolite, the non-standardized and standardized mean-tensors are similarly oriented and show quite orthorhombic confidence cones (Fig. 3a and b). This suggests that their AMS fabrics, of higher and of lower susceptibility minerals are coaxial, perhaps because these represent distal, off-axis mantle flow. In contrast, closer to the spreading axes, the mantle sequence rocks of the Troodos ophiolite massif, 30 km to the east indicate some non-coaxiality in the fabric development (Fig. 5a and b) (Borradaile and Lagroix, 2001). At Akamas and at Troodos, the foliations dip eastwards and the mineral extension, approximated by the orientation of the maximum susceptibility axis, plunges gently south. When the specimens are standardized, the plunge of the maximum susceptibility is less, suggesting that the subfabric of high susceptibility phases is more steeply aligned. This is confirmed in the next section, where the subfabric of magnetite-titanomagnetite is isolated from the anisotropy of their remanence. Of course, ilmenite's contribution cannot be isolated; although it is a high susceptibility accessory, it does not carry a remanence under any temperatures realised in the earth (e.g. Dunlop and Özdemir, 1997).

We must recall that the shapes of individual specimen-tensors, usually described by the anisotropy parameters P_j and T_j (Jelinek, 1981), are not directly related to the fabric inferred from the orientation-distribution of principal axes. After all, structural geologists are aware that platy minerals may be arranged with their normals in a zone-axis girdle to define an L-fabric. Platy minerals need not define an S-fabric and acicular minerals need not define an L-fabric (Flinn, 1962, 1965). Similarly, the tensor-ellipsoid shapes of individual specimens need not correspond to the shape of the orientation-distribution ellipsoid. The latter is best placed in the L–S scheme by inspecting the orientation-distribution of principal axes of all specimens on a stereogram or the shapes of the confidence cones for the mean-tensor. Specimen-AMS ellipsoid shapes are shown in the Jelinek fabric plot (Fig. 4a) from which it is clear that oblate-shapes predominate ($+1 > T_j > 0$) with a

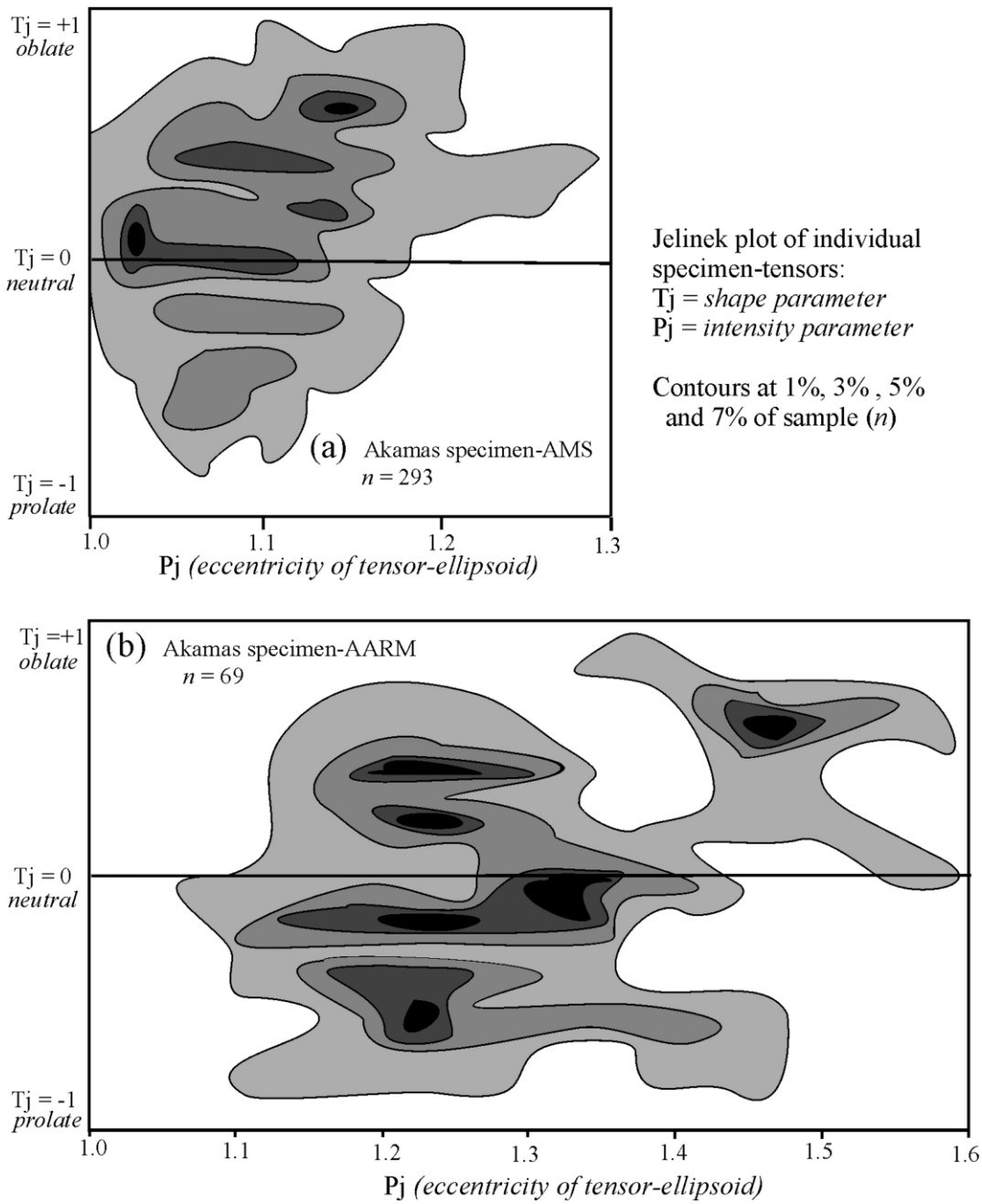

Fig. 4. The Jelinek (1981) plot of P_j (eccentricity) against shape (-1 = prolate $\leq T_j \leq +1$ = oblate) is shown for both AMS and AARM in the Akamas mantle-sequence rocks. This is valid only for specimen-tensors. The *shape of the orientation-distribution ellipsoid* of susceptibility tensors is inferred from stereographic projections of the principal magnetic fabric axes of specimen tensors (e.g. Figs. 3 and 5). Here, the Jelinek-plot shows the shapes of tensor-ellipsoids for individual specimens. (a) AMS *specimen-anisotropy* is mostly neutral to weakly-oblate ($0 \leq T_j \leq +1$), as is common for mafic silicates whose AMS is *crystallographic*ally controlled. The low eccentricity, mostly $P_j \leq 1.2$, is also typical. (b) AARM *specimen-anisotropy* indicates the specimen anisotropy of magnetite in these specimens. It is typical that this shows higher eccentricity ($1.1 \leq P_j \leq 1.6$) and more commonly prolate shapes ($T_j \leq 0$), due to the *shape*-controlled anisotropy of magnetite.

concentration near neutral ellipsoid-shapes ($T_j \sim 0$). The eccentricities of AMS ellipsoids are modest, mostly with $P_j < 1.2$ ($P_j = 1$ for a sphere). Specimen-anisotropies are a subdued version of the anisotropy of the mineral-phase that dominates the AMS, in terms of both anisotropy and bulk-susceptibility. By comparing these specimen anisotropies with those of individual minerals collected from the main Troodos harzburgite, one recognises that pyroxenes and serpentine mainly control AMS, their susceptibilities enhanced by lattice-aligned magnetite inclusions (Lagroix and Borradaile, 2001).

4.2. AARM: anisotropy of anhysteretic remanence

Anisotropy of remanence must be determined from artificial remanences acquired in low fields, e.g. $\leq$0.1 mT,

to ensure a linear relation between magnetization and field (Dunlop and Özdemir, 1997) that permits calculation of a second-rank tensor. The tensor is calculated from the weak permanent magnetizations that are successively applied along different axes through the specimen. Of course, it must be possible to erase each artificial remanence before the next one is applied, along a different direction through the specimen. For many technical reasons, the most suitable type of artificial remanence is anhysteretic remanence (ARM) and its anisotropy therefore takes the acronym AARM. It is possible to determine another kind of remanence-anisotropy with the technically simpler artificial isothermal remanent magnetization (IRM). However, larger fields are necessary to produce intensities of sufficient magnitude and care is required to ensure that there is a linear response between fields and magnetization (Daly and Zinsser, 1973; Borradaile and Dehls, 1993; Jelinek, 1996). AARM is more demanding, in terms of time, equipment and specimen selection but far superior. The technique was introduced by McCabe et al. (1985) and is reviewed explicitly by Jackson (1991) and it has the interesting potential that it may be refined to isolate further subfabrics of different grain-size within the magnetite-subfabric (Jackson et al., 1989; Nakamura and Borradaile, 2001a,b).

AARM determination is somewhat more involved than that for AMS. Each anisotropy-determination requires for seven-measurements of successive ARMs, applied in different directions, using the procedure and software we have developed. The cylindrical core is given an ARM along each of the same seven axes used in AMS. After each permanent magnetization, its remanent magnetization is measured and then cleaned by AF demagnetization before a subsequent ARM is applied and measured along the next direction. From the seven remanences, anisotropy of remanence is determined, represented by an ellipsoid, just as with AMS. Anhysteretic remanence has the advantage that a suitably large magnetization-intensity is achieved in the presence of a low direct field. This is possible because the weak direct magnetizing field is applied concurrently with a large alternating field that leaves no permanent effects but mobilizes spin-moments, permitting them to be strongly aligned by the weak DC field. In this study, we used an AF that decayed from a peak value of 100 mT and activated the DC field over the window from 80 to 0 mT. Applying and measuring the ARMs along the seven-axis orientation sequence of Borradaile and Stupavsky (1995) has the technical advantage that successive ARM applications usually erase the preceding remanence, so that a full three-axis demagnetization between each ARM is not always needed (software alerts the user to this possibility). The success of each ARM application technique is apparent when it is acquired closely parallel to the applied field direction. We used a Molspin spinner magnetometer with the acquisition and control software SPIN01.exe to measure the ARMs imposed in different directions and to determine the anisotropy of remanence from them (AARM).

AARM was determined for one specimen from each outcrop of the Akamas mantle sequence rocks and the orientation distribution of their A_{MAX} and A_{MIN} axes is shown in contoured density plots (Fig. 3, lower left insets). The orientation distributions are satisfactorily unimodal, validating the calculation of the mean tensor and the confidence cones for its principal axes (Fig. 3c and d). In a similar manner to AMS, the specimen-tensors may be standardized to reduce the effect of specimens that have both high remanence-intensity and anomalous fabric-orientation. This usually enhances the precision with which the AARM fabric is defined by reducing the size of the confidence cones around the principal axes (Fig. 3d). However, the confidence cones become non-orthorhombic in this case, being asymmetrical with respect to the magnetic foliation. Either the sample-size ($n = 69$) is inadequate to define a stable orientation-distribution or, more probably, two subfabrics of magnetite-titanomagnetite accessory minerals are present (e.g. Borradaile and Gauthier, 2003). In the latter case, their anhysteretic remanence-intensities are too similar for distinction by standardization of the specimen-tensors because neither subfabric constitutes a statistical outlier in the orientation-distribution. AARM reveals an easterly dipping foliation of the ferromagnetic subfabric with a NE mineral lineation (Fig. 3c and d). The larger sample studied in the main exposure of Cretaceous mantle sequence, at Troodos, also shows an easterly dipping foliation but also an east-plunging mineral lineation (Fig. 5c and d).

Individual specimen-anisotropy ellipsoids are much more anisotropic than for AMS ranging from eccentricities of $1.1 \leq P_j \leq 1.6$ (Fig. 4b), a typical feature of remanence-anisotropies. More important, the shapes are mostly prolate, a common feature for magnetite-titanomagnetite grain-shapes.

4.3. Comparison of Akamas magnetic fabrics with those of the Troodos mantle-sequence

The mantle-sequence rocks of the Troodos ophiolite, exposed in the up-domed centre of the complex, near Mount Olympus, are similar in appearance and petrography to the mantle sequence rocks at Akamas. Although the Akamas rocks are more sheared and more fractured their penetrative fabrics are rather similar in orientation. The AMS fabrics, especially those for standardized specimen tensors, reflect the orientation distribution of matrix silicates; at Troodos and Akamas, foliations dip eastwards, more gently at Troodos. The mineral lineations plunge very gently, almost N–S. The shape of the orientation distribution, as revealed by the shapes of mean-tensor confidence cones, is designated $S > L$ in both regions. Of course, Flinn's (1965) L–S scheme is here applied to the orientation-distribution; it is unrelated to the shapes of the specimen tensor-ellipsoids.

AARM foliations also dip eastwards in both regions, but

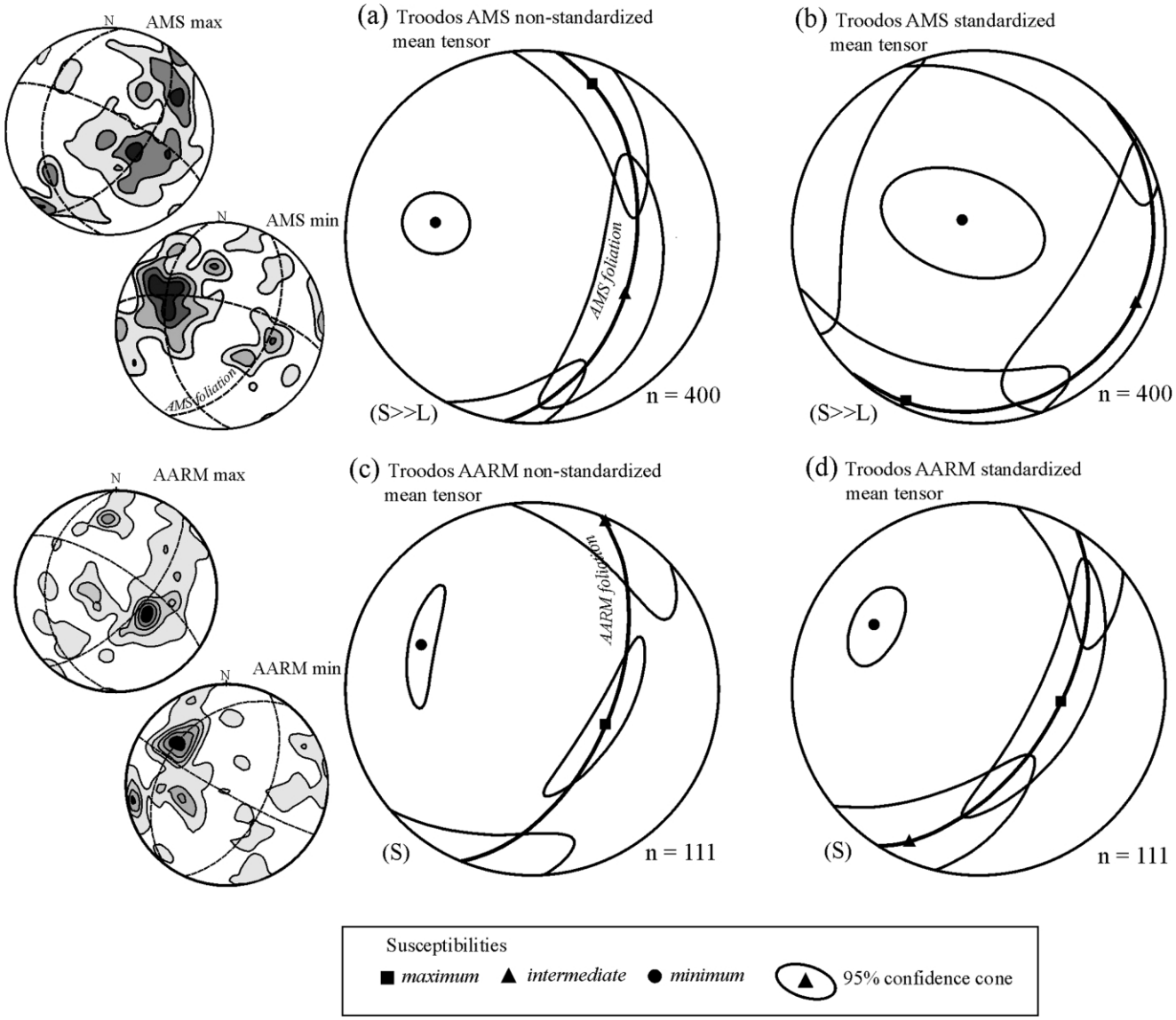

Fig. 5. Magnetic fabrics from the main inlier of mantle-sequence rocks near Mount Troodos (Fig. 1). Note the similarity in orientation of the principal fabric elements to those at Akamas, with an easterly dipping foliation, and N–S mineral lineations for both AMS (a, b) and AARM (c, d).

differently from their AMS foliations. However, AARM-defined mineral lineations indicate that the remanence-bearing accessory minerals plunge NNE at Akamas but easterly at Troodos. The small differences in orientations of the mean AMS fabrics between Akamas and Troodos further confirm the view that they belong to the same tectonic unit, sharing the same patterns of primary mantle flow. The small differences in orientation and shape of the orientation-distribution ellipsoid are compatible with a more distal, off-axis solidification of the Akamas ophiolite.

The standardized AARM fabrics of Akamas and Troodos show greater similarities in orientation than their AMS fabrics. This may be understandable since they demonstrate the orientation distributions of a younger subfabric, acquired at a later stage in the non-coaxial deformation process. In both regions the shape of the orientation distribution ellipsoid is $S \geq L$ for AMS but the AARM fabrics show $S < L$ at Akamas, whereas the fabrics are planar (S) at Troodos. The differences in fabric shape may be compatible with better definition of the flow-alignment further from the spreading axis.

5. Paleomagnetic results

5.1. Paleomagnetism

Our paleomagnetic results were obtained from the same cylindrical cores used for AMS. Whereas AMS does not disturb the natural remanent magnetisation (NRM), AARM destroys it, so that cores used for AARM were not studied further paleomagnetically. Remanence was measured mostly in a Molspin spinner magnetometer, the higher-sensitivity JR5a unit not normally being required. The

software package SPIN01.exe was used for data acquisition, management and interpretation. Significant remanence components were isolated by incremental demagnetization, re-measuring the remanence after each step. Significant turning points in the vector-plot separated the main vector components, a single secondary, B-component and a characteristic A-component that is stable to the point of complete demagnetization. We employed three steps of low-temperature demagnetization followed by at least 11 steps of thermal demagnetization using the automated, Shaw-TM80 thermal demagnetizer. We have found low temperature demagnetization (LTD) particularly effective in reducing the overlap of unblocking-temperature spectra between different vector components (Borradaile et al., 2001, 2003). It yields straighter vector components, separated by sharper turning points. Characteristic components (ChRMs) were isolated by principal-component analysis using five or more turning points (Kirschvink, 1980). LTD requires cooling the samples in liquid Nitrogen (77 K) and allowing them to warm back to room temperature in a magnetic shield. The specimens cycle through a magnetic-crystallographic transition at ~120 K, which erases less significant, 'soft' magnetization associated with domain-walls in multidomain magnetite (Dunlop and Özdemir, 1997; Muxworthy et al., 2003). Subsequent, traditional thermal demagnetization then more successfully isolates the ChRMs.

Curie-balance work, using a Sapphire Instruments horizontal-translation balance, confirmed that magnetite is the ubiquitous and most significant remanence carrying phase, both in the Akamas mantle-sequence rocks (Fig. 6a and b) and in the Troodos main outcrop of mantle-sequence harzburgites (Borradaile and Lagroix, 2001). However, the thermomagnetic curves for Akamas specimens are straight in comparison with those of the fresh harzburgite of the main Troodos outcrop, near Mt. Olympus. The Akamas curves are more similar to the severely altered harzburgites of Troodos, in which the olivine was replaced by iddingsite and hematite (Borradaile and Lagroix, 2001). It is therefore understandable that the more sheared Akamas harzburgite shows this sub-paramagnetic, uniform-gradient, Curie-curve, with magnetite as the prominent phase losing remanence at a Curie-temperature of ~580 °C. In some instances, a still lower Curie-temperature is observed, ~350 °C perhaps attributable to a titanomaghemite phase. We have found this elsewhere in the Troodos ophiolite, especially altered sheeted dikes that overly the mantle sequence and show more extensive oxidation and sea-floor hydrothermal-metamorphism (Fig. 6c). That produces titanomaghemite, an oxidized form of the sea-floor stable oxide, TM_{60}, to which we attribute the ~350 °C Curie-temperature (e.g. Borradaile and Gauthier, 2003).

Every paleomagnetic specimen was subject to the same full incremental demagnetization treatment, involving three steps of low-temperature demagnetization and at least 10 steps of thermal demagnetization. A typical treatment is shown in the vector plot of Fig. 7. Our interactive software permitted us to review the data immediately in rotatable, three-dimensional vector-plots (Fig. 7a). After this inspection, we were easily able to recognise the presence of separate components, their relative stability and the important turning-points that correspond to key unblocking temperatures. The vector endpoints required by the principal-component calculation are then selected from conventional two-dimensional vector-plots (Fig. 7b–d) (Zijderveld, 1967). An intensity-decay plot verifies unblocking temperatures (T_{UB}), which mostly show a secondary component unblocking at ~350 °C (Fig. 6e). Secondary and characteristic directions obtained by principal component analysis are then presented in stereograms (Figs. 8 and 9).

In almost every specimen, only one secondary, B-component and the primary A-component are identified. The most surprising feature is their simplicity and geographical uniformity, as with a further 600 still unpublished paleomagnetic results acquired by our laboratory for the Troodos dike complex. In part, this is due to the good fortune of the Late Cretaceous 'quiet' magnetic period of constant normal polarity (Fig. 11c), during which most Troodos rocks acquired their magnetizations. However, it is also in no small part due to the simple deformation of most Troodos microplate, as well as a rather simple post-magnetization deformation history for much of the Mamonia terrane. (Our work shows that most Mamonia paleomagnetic records are due to post-deformation chemical remanences although that is also generally known from the paleomagnetism of penetratively deformed rocks.)

Our paleomagnetic data from Akamas has been particularly easy to evaluate for two reasons. First, we have benefited from the use of incremental demagnetization for every specimen, not just of pilot studies. Second, we used low-temperature demagnetization to reduce overlap of unblocking spectra of different vector-components during the ensuing campaigns of thermal or AF incremental demagnetization. This leads to the recognition of very well-defined A-components and B-components and shows that the exposures of the Akamas mantle sequence behaved as a coherent tectonic unit since the A-component was acquired (Fig. 8a and b). Both components are reversed in polarity.

5.2. Comparison of paleomagnetic results with the main Troodos ophiolite mantle-sequence

The mantle-sequence rocks near Mt. Olympus, in the main Troodos ophiolite, also show just an A- and a B-component, but the B-component unblocking temperatures are higher than for the Akamas ophiolite (Fig. 8c, cf. Fig. 9e). A-components and B-components are mostly normal polarity around Mt. Olympus, but less well-defined reversed-polarities are found also (Fig. 9b and d). Reverse polarities are recorded elsewhere in the Troodos ophiolite as

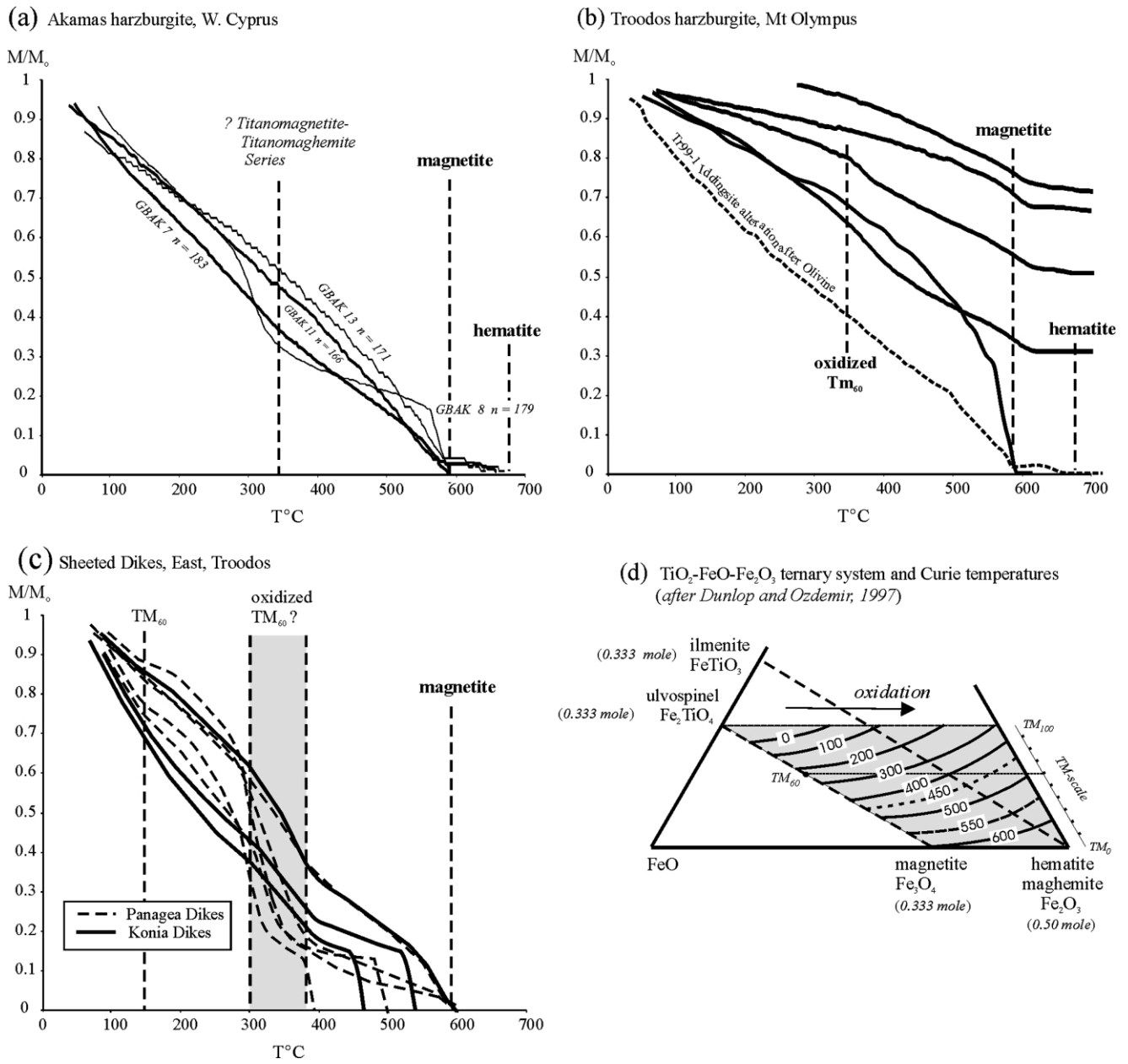

Fig. 6. Curie-balance tests reveal the characteristic Curie temperatures of magnetite in all specimens (~580 °C) as well as a Curie temperature that is appropriate for TM60 (~150 °C) or its oxidized counterpart (~360 °C), and hematite (~670 °C). (a) Akamas harzburgites. (b) Troodos harzburgites, from the main Troodos outcrops near Mt. Olympus. (c) Sheeted dikes in the Troodos complex ophiolite, east of Mt. Olympus. Extensive sea-floor metamorphism and alteration caused replacement of magnetite and TM_{60} by oxidized TM-group minerals (e.g. titanomaghemite). (d) Part of the ternary diagram of titaniferous iron-oxides with approximate Curie-temperatures contoured (after Dunlop and Özdemir, 1997). The horizontal line to the right of TM_{60} shows the compositions and Curie-temperatures of more oxidized versions.

an expected consequence of lateral ocean-floor spreading during polarity switches (e.g. Gee et al., 1993); for the most part shallow ophiolite acquires thermochemical remanences off-axis rather than as simple thermal remanences acquired by magmatic cooling. Characteristic remanence directions at both Akamas and Mt. Olympus are similar, and not too different from the present geomagnetic field or its reversed equivalent. This could suggest that the magnetizations are relatively young, associated with Tertiary uplift but a more reliable and sensitive comparison is possible if the paleopole-locations responsible for these magnetizations are compared with others from Cyprus.

Previously determined paleomagnetic vectors were rarely presented in three-dimensions on stereograms, but a convincing argument for the clockwise rotation of the Troodos microplate was made by tabling paleomagnetic-declinations against the age of the source formation (Clube and Robertson, 1986, their Table 1), by graphing declination against age (Morris, 1996) or by time-designated declinations on a rose-diagram (Lagroix and Borradaile, 2000).

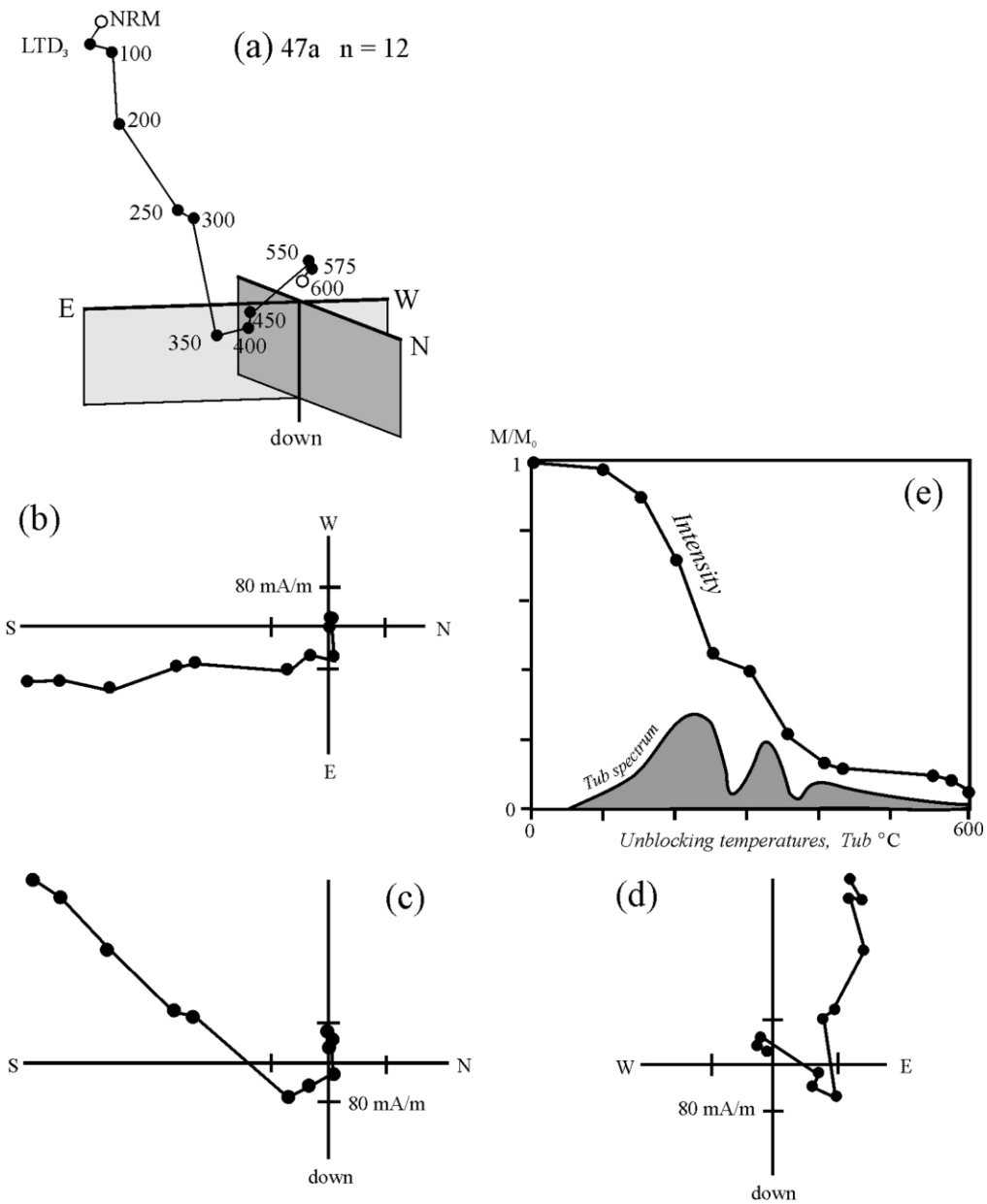

Fig. 7. Demagnetization graphs of a typical Akamas harzburgite. (a) Three-dimensional vector plot, rotatable on computer monitor to permit rapid recognition of stable vector components (i.e. five or more vector-end-points in line defined by principal component analysis; Kirschvink, 1980). NRM = initial magnetization; LTD_3 = after three steps of low-temperature demagnetization cycling in liquid-nitrogen. Remaining thermal demagnetization steps in C°. Every sample was processed using this full demagnetization treatment, at Akamas and Troodos. (b–d) More traditional two-dimensional vector plots. (e) Plot of decay of magnetic intensity, with unblocking temperature spectrum.

Although not previously used in studies of Cyprus, the traditional paleomagnetic approach of calculating the location of the magnetic north-pole responsible for the magnetization is much more revealing (e.g. van der Voo, 1993). It is the fullest possible inverse-expression of the site's motion relative to the North magnetic pole from which one may estimate the location of the vertical rotation-axis responsible for various microplate motions, latitudinal changes and relative longitudinal changes. A large number of paleomagnetic vectors have been published for the Troodos Complex (original data and summary of previous work by Clube and Robertson, 1986; Table 1, 1314 vectors), Akamas (our data; Table 2, 153 vectors), and from the Mamonia terrane (Morris et al., 1998; Table 3, 156 vectors). Most of these vectors are of high precision but since this regional interpretation requires the original data to be grouped into generalized site-means or formations-means, some of the confidence cones we use are conservative (Fig. 10b; Table 4). This is partly the cause of the rather low quality ranking of the paleopoles, using current criteria (van der Voo, 1993; Scalera et al., 1996). It is not always easy to verify the primary nature of paleomagnetic data in Cyprus

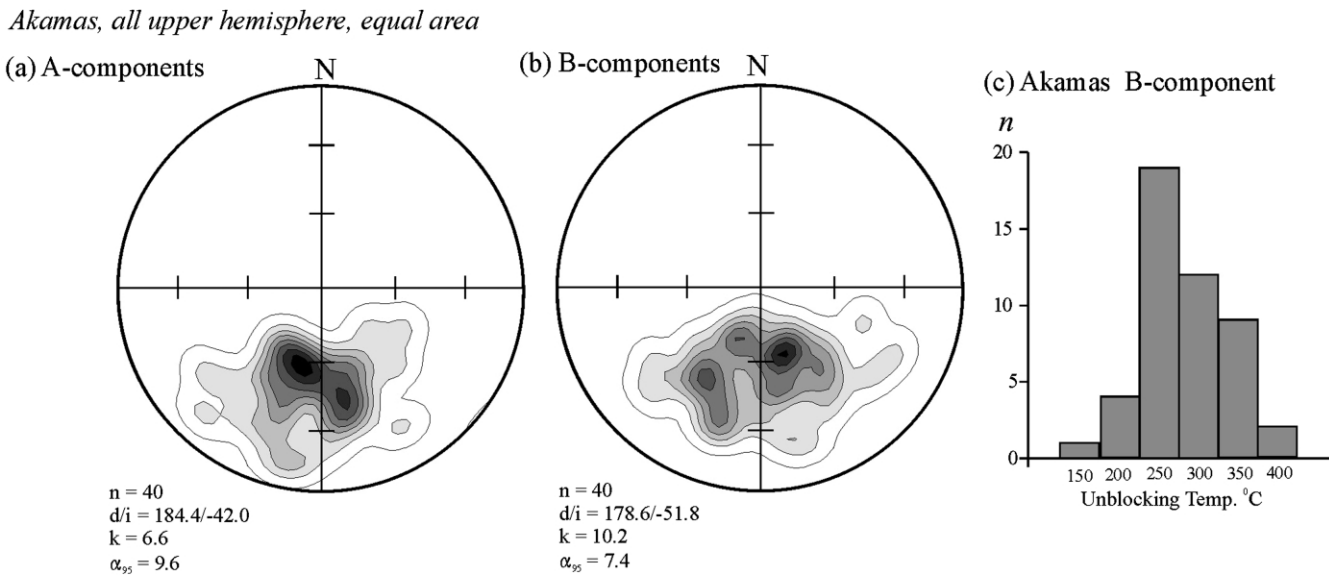

Fig. 8. Stable vector-components identified from demagnetization-plots, such as in the preceding figure, reveal two stable components in all specimens from Akamas. All remanences are upwards-seeking, having been acquired during a reversed geomagnetic polarity, and are plotted on the upper hemisphere. (a) The last stable vector component to be removed, which decays close to the origin of the vector-plot, represents the oldest or A-component. (b) The first component to demagnetize (B-component) represents the younger magnetization. (c) Frequency-distribution of the unblocking temperatures of the B-component.

using reversal-symmetry or conglomerate tests although there are exceptions, e.g. fold tests of Morris et al. (1998). However, lithologies and tectonic setting indicate that remanences are largely depositional in the case of the limestones and chemical or thermochemical in the case of the sheeted dikes and pillow lavas. The deeper ophiolite members, the mantle sequence rocks, especially near Mt. Olympus may possess simpler thermal remanences blocked in during uplift. The Formation-mean vectors from Table 1 do not provide a very broad spread of paleopoles (Fig. 10a). However, paleopoles from the original site-mean data, and our new data from Akamas (Tables 2 and 3) and from the earlier literature elsewhere in Cyprus (Table 4) form a broad sweeping locus (Fig. 10b). We propose that it is reasonable to consider this as a tentative APWP for several reasons. First, the well-accepted vertical axis-rotation of Cyprus was based solely on the comparison of paleomagnetic declinations (Clube et al., 1985). Taking further advantage of the paleomagnetic data here, by also using the inclinations merely establishes the veracity of that rotation in terms of our proposed APWP (Fig. 10b). Moreover, this is confirmed with the benefit of more recently acquired data (Table 4). From those site mean vectors, we determined paleopoles that lie on an arc of progressive age, in a clockwise sense, confirming not only the anticlockwise rotation of Cyprus but also its changes in paleolatitude, evident by comparing the paleopoles with the lines of co-latitude around Cyprus (Fig. 10). One may argue that errors are introduced by omitting tilt-corrections, or by the use of site-means that obscure them. However, this did not deter the first recognition of the rotation of the Troodos microplate, and the tenacious acceptance of a 'Troodos mean vector' in the earlier

Table 1
Paleopoles calculated from published formation-mean paleomagnetic vectors for Cyprus-Troodos microplate and for the Akamas peninsula (mean site location: 35°N, 33°E)

Age (Ma)	Formation and polarity (N or R)	n	Mean decrease	Mean increase	α_{95}	Paleopole	
						Latitude	Longitude
~88	Turonian; Troodos extrusives	663	274.0	36.0	12.3	14.1	316.7
~88	Turonian; Akamas ophiolite	217	276.0	41.0	14.1	17.6	318.8
~88	Turonian; basal umbers	56	279.0	6.0	28.6	9.1	299.4
80–75	Campanian limestones	25	289.0	13.0	23.9	19.4	296.7
72–55	Maastrichtian–Paleocene (normal)	116	336.0	32.0	13.2	62.8	270.2
72–55	Maastrictian–Paleocene (reversed)	101	152.0	−14.0	15.3	52.7	262.2
<55	Lower Eocene	136	357.0	38.0	10.1	77	224.5

A comprehensive summary of previously determined vectors may be found in Clube and Robertson (1986) with original sources primarily in Abrahamsen and Schönharting (1987), Allerton (1989), Allerton and Vine (1990), Bonhommet et al. (1988), Clube et al. (1985), Hurst et al. (1992), MacLeod et al. (1990), Morris et al. (1990, 1998) and Varga et al. (1999). n = number of characteristic stable vectors, Fisher means with α_{95} calculated assuming Fisher statistical model.

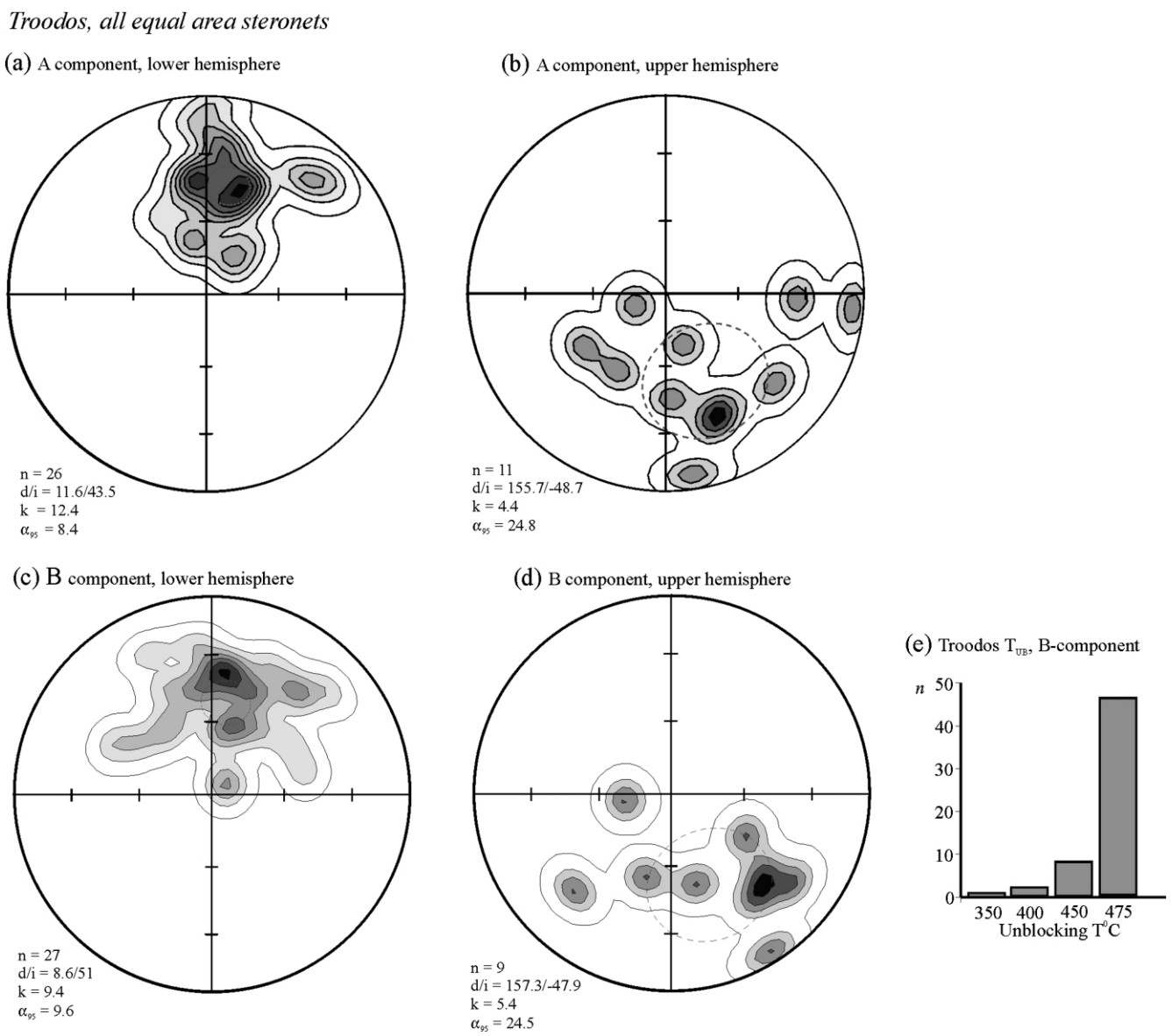

Fig. 9. Stable vector components of A- and B-component remanences from the main mantle-sequence exposures near Mt.Troodos. Both downwards-seeking magnetizations (a, b; lower hemispheres) and upwards-seeking magnetizations (c, d; upper hemispheres) were acquired during normal and reversed polarity, respectively. (e) Unblocking temperatures of the B-component are typically much higher than in the Akamas mantle-sequence (see preceding figure).

Table 2
This paper: new paleomagnetic data, Akamas and Troodos mantle-sequence ophiolite, Cyprus Akamas (mean site location: 35°00′N, 32°20′E)

Mode and Polarity	*n*	Mean decrease	Mean increase	α_{95}	*k*	Paleopole	
						Latitude	Longitude
Akamas-A-reversed	40	184.4	−42	9.6	6.6	79.5	189.4
Akamas-B-reversed	40	178.6	−51.8	7.4	10.2	88	249.1
Troodos-A-normal	26	11.6	43.5	8.4	12.4	76.7	159.5
Troodos-A-reversed	11	155.7	*−48.7*	24.8	4.4	68.9	296.7
Troodos-B-normal	27	8.6	51	9.6	9.4	82.4	137.3
Troodos-B-reversed	9	157.3	*−47.9*	24.5	5.4	70	293.5

n = number of characteristic stable vectors, Fisher means with α_{95} calculated assuming Fisher statistical model. *k* = Fisher concentration parameter.

Table 3
Mamonia paleopoles calculated from the vectors in Morris et al. (1998) for the Akamas peninsula (mean site location: 35°00′N, 32°30′E)

Mode and polarity	n	Mean decrease	Mean increase	α_{95}	k	Paleopole	
						Latitude	Longitude
CY18 (Morris et al., 1998)	10	9.4	−22.3	2.1	539	−11.6	19.2
CY20 (Morris et al., 1998)	7	28.4	−14.1	3.9	245	−7.2	353.4
CY22 (Morris et al., 1998)	9	41.5	−5.6	8.2	41	−2.9	336.7
CY21 (Morris et al., 1998)	5	51.1	1.3	4.6	273	0.6	145.7
CY17 (Morris et al., 1998)	8	323.4	−40.5	5.8	91	−23.2	68.5
CY15 (Morris et al., 1998)	8	299.9	−52.3	5.2	113	−32.9	78.7
CY16 (Morris et al., 1998)	6	306.2	−49.1	5.1	173	−30	76.9
CY23 (Morris et al., 1998)	6	250.7	−54.1	8.9	57	−34.7	99.6
CY27 (Morris et al., 1998)	5	253.9	−57.7	2.5	933	−38.4	94.4
CY25 (Morris et al., 1998)	5	304.5	−28.4	13.2	35	−15.2	88.7
CY26 (Morris et al., 1998)	8	300	−35.7	4.1	184	−19.8	88.3
CY01 (Morris et al., 1998)	8	247	−6.5	8.6	42	−3.3	132.5
CY02 (Morris et al., 1998)	6	256.6	−6	5.5	151	−3.1	127
CY03 (Morris et al., 1998)	3	259.4	−10.9	5.5	502	−5.5	123.3
N. Akamas (Clube et al., 1985)	62	280.2	4.1	3.5	28	2	297.9

n = number of characteristic stable vectors, Fisher means with α_{95} calculated assuming Fisher statistical model. k = Fisher concentration parameter.

literature was so great that some workers even untilted their vectors so as to agree with that very generalized formation mean vector (~274/ + 36). In this project, we avoid the use of tilt-corrections since, in most cases, the adjustments would not justify the errors that could be induced. For example, not knowing the actual original tilt axis, there is always an ambiguity concerning the declination of the untilted vector derived from stratified formations (MacDonald, 1980). This situation is worse for dikes in which an unknown rotation axis leads to an ambiguity of both declination and inclination (Borradaile, 2001b). The non-commutative nature of natural rotations sequences means that the required knowledge of the sequence of component tilts may never be known (Borradaile, 1997) and we therefore recommend that it is better not to correct for small rigid body tectonic tilts here.

The paleopole locations calculated for the Troodos microplate, for the Mamonia terrane and for our new data from Akamas lie on a single arc (Tables 1–4; Fig. 10). It is highly improbable that localized tilting and faulting has conspired to cause paleopoles of different ages to form such a structured pattern. The simpler and more logical explanation is that the internally consistent pattern represents an apparent polar wander path (APWP) due to microplate motion, despite any imprecision due to the absence of corrections for tectonic tilting.

In Fig. 10, we may compare the Troodos APWP with lines of colatitude around Cyprus. These show that Cyprus was ~90° latitude south of the pole (equatorial) during the early part of the rotation (88–55 Ma). It moved south of the equator briefly at ~60 Ma and then moved quickly north to its present latitude (34°N), with rotation apparently slower in the last 15 Ma. The vertical rotation-axis of the Troodos microplate may have been within the microplate, as previously inferred (Clube and Robertson, 1986), but only until ~60 Ma, after which the APWP takes a turn and cuts across the lines of colatitude bringing the microplate closer to the North pole. The overall rotation of the Troodos microplate slightly exceeded 90° anticlockwise, about two-thirds of the rotation being completed in the interval 88–65 Ma at an almost equatorial paleolatitude.

The adjacent Triassic Mamonia terrane had an independent tectonic history before it was sutured to the Cretaceous Troodos microplate. Ophiolites within the Mamonia terrane crop out along arcuate fault-bounded zones that are approximately concentric about the centre of the Troodos microplate. Since they are associated with Triassic sedimentary rocks, it was proposed that they represent Triassic ocean floor, juxtaposed with the Cretaceous Troodos-plate ophiolite by the subduction of intervening Jurassic ocean floor. However, Robertson and Woodcock (1979, p. 664) noted this is unnecessary since rotation of the Troodos microplate above the subduction zone could have brought it into contact with Triassic ophiolite of northern provenance (Clube and Robertson, 1986, their fig. 15; see Fig. 12 here). Moreover, recent mapping of the penetratively deformed Mamonia ophiolite fragments suggest they may be fragments of the Troodos terrane, incorporated into the Mamonia terrane when the microplates sutured (Bailey et al., 2000). The uncertainty is not strictly important, from the view of paleomagnetism, because the characteristic remanences of strained rocks invariably postdate penetrative deformation. Thus, the very high quality paleomagnetic vectors isolated by Morris et al. (1998) may be used to calculate the Mamonia APWP, after the penetrative deformation of its included ophiolites. Our calculations of their paleopoles (Table 3), extend the arc of our APWP determined for the Troodos terrane (Fig. 10c). It shows clear evidence of Mamonia-terrane rotation through an arc of ≥90°. Unfortunately, the relative ages of the sites'

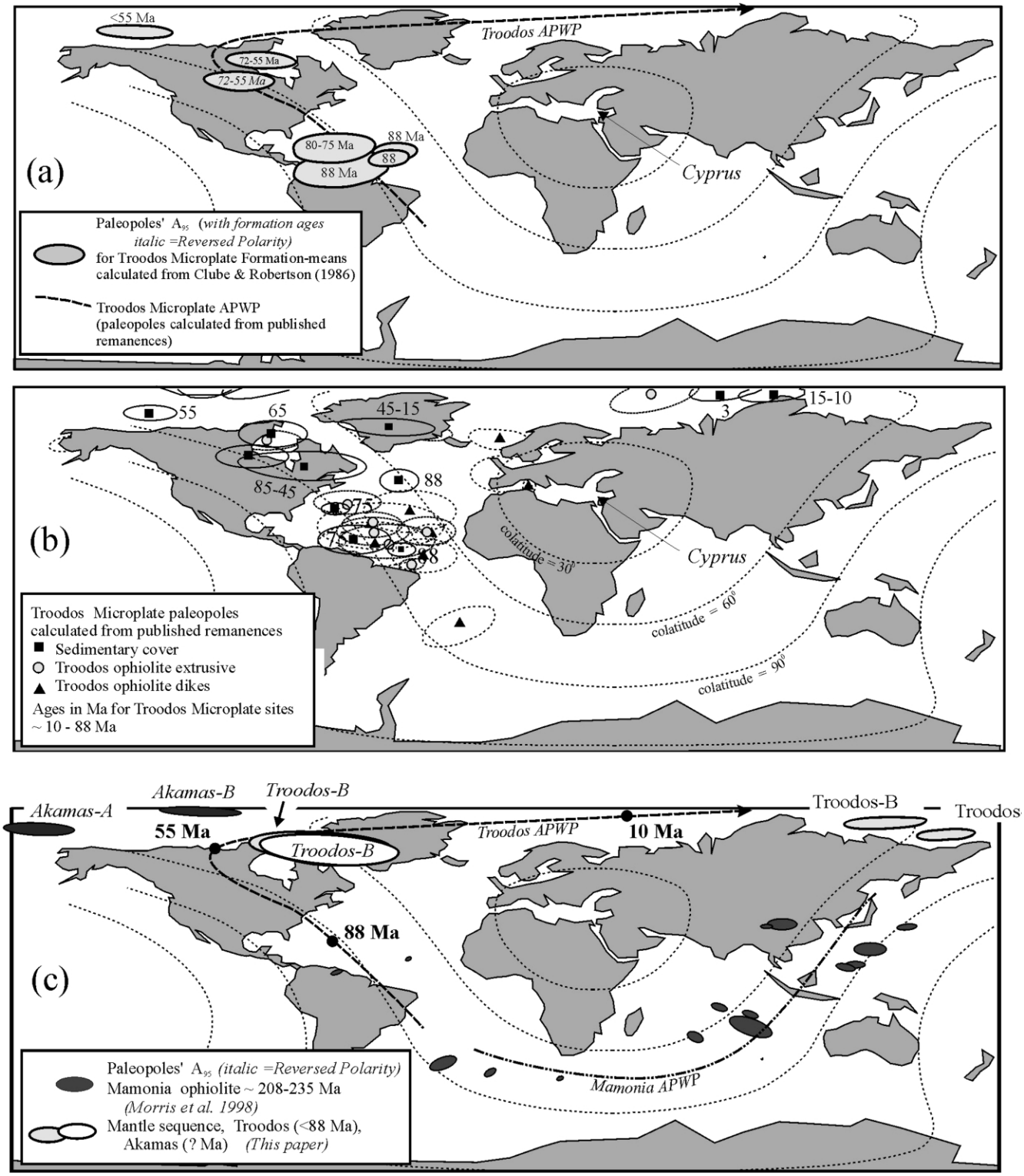

Fig. 10. Paleopole locations (note distortion at high-latitude due to map-projection). (a) For the Troodos-microplate, calculated from the formation-mean vectors of Clube and Robertson (1986). (b) For all published data, using individual site-means from published characteristic remanences given in Table 4. (c) Akamas and Troodos paleopole locations from the new data of this paper and the Mamonia-terrane paleopoles that we calculated from the high-quality paleomagnetic data (individual sites) of Morris et al. (1998). Tentative apparent polar wander paths (APWP) for the Troodos microplate and for the Mamonia terrane are shown.

Table 4
Paleopoles determined from published paleomagnetic vectors

Reference	Quality		Unit	Age	Sites		Demagnetisation		Mean vector (Fisher)			Paleopole			
Ref	V	S		Ma	*N*	*n*			Dec.	Inc.	α_{95}	Lat.	Long.	dm	dp
4	2	A	Lmstn	15–45	14	38	T/AF	M	336.0	56.0	15.0	70.5	314.5	8.8	5.5
4	2	A	Lmstn	45–85	11	26	T/AF	M	322.0	30.0	26.0	51.1	283.7	24.9	13.0
1	4	B	Lmstn	65	5	116	AF	1	336.0	32.0	13.2	62.2	269.6	12.5	6.5
1	4	B	Lmstn	65	6	101	AF	1	152.0	−4.0	15.3	52.0	262.2	15.1	7.6
1	4	B	Lmstn	55	5	136	AF	1	357.0	38.0	10.1	76.0	224.6	9.4	5.0
2	3	B	Lmstn	75	1	25	AF	1	289.0	13.0	23.0	19.3	297.4	23.7	11.9
3	2	B	Lmstn	75	1	8	AF	M	306.0	20.0	7.0	35.1	289.9	6.8	3.5
5	2	A	UPL	88–91	1	9	T/AF	M	273.0	50.0	19.0	19.2	327.6	16.3	9.5
5	4	A	LPL	88–91	1	5	T/AF	M	284.0	26.0	21.0	19.1	306.5	20.4	10.5
5	4	A	LPL	88–91	1	6	T/AF	M	262.0	33.0	9.0	3.9	323.2	8.5	4.5
5	4	A	LPL	88–91	1	6	T/AF	M	298.0	25.0	20.0	30.3	297.9	19.4	10.0
5	2	A	BG	88–91	1	5	T/AFM	M	2.0	59.0	15.0	84.9	50.8	11.5	7.5
5	2	A	BG	88–91	1	7	T/AFM	M	337.0	13.0	7.0	54.5	255.0	6.9	3.5
5	2	A	SD	88–91	1	6	T/AF	M	9.0	32.0	8.0	70.6	186.2	7.6	4.0
6	2	B	SD	88–91	14	81	AF	1	42.0	60.0	12.3	56.6	100.0	9.2	6.1
6	2	B	SD	88–91	18	116	AF	1	348.0	69.0	9.5	70.5	10.6	5.7	4.7
6	1	B	SD	88–91	4	8	AF	1	274.0	37.0	21.7	14.8	318.0	20.3	10.8
6	1	B	SD	88–91	8	48	AF	1	297.0	30.0	36.4	31.0	301.4	34.9	18.2
6	1	B	SD	88–91	8	46	AF	1	288.0	17.0	33.1	19.6	299.8	32.7	16.5
7	1	B	SD	88–91	13	108	T	1	342.0	64.0	14.0	72.6	346.5	9.7	7.0
8	0	B	SD	88–91	32	52	AF	1	314.0	70.0	26.7	52.9	348.2	15.7	13.3
8	1	B	SD	88–91	43	66	AF	1	11.0	74.0	5.1	63.8	45.4	2.5	2.5
9	1	C	SD	88–91	19	110	T/AF	1	310.0	74.0	5.9	49.4	357.1	2.9	2.9
10	2	B	BG	88–91	4	25	AF	M	328.0	61.0	12.6	64.1	328.4	9.3	6.3
10	2	B	BG/LPL	88–91	4	72	AF	M	335.0	28.0	15.3	59.8	267.4	14.7	7.6
10	4	B	UPL	88–91	4	28	AF	M	279.0	0.0	7.0	7.3	297.8	7.0	3.5
10	3	B	PL/BG	88–91	4	44	AF	M	279.0	21.0	21.0	13.5	306.9	20.6	10.5
10	2	B	Umber	88?	11	11	AF	M	304.0	52.0	4.5	44.0	317.9	3.7	2.2
2	3	B	Umber	88–91	5	56	AF	1	279.0	6.0	28.0	9.0	300.2	27.9	14.0
11	1	B	SD	88–91	9	45	AF	1	299.0	46.0	28.4	38.0	312.4	25.2	14.1
11	1	B	SD	88–91	15	87	AF	1	239.0	23.0	24.2	−7.1	331.6	23.6	12.1
11	2	B	SD	88–91	39	162	AF	1.0	19.0	64.0	9.1	72.0	80.5	6.3	4.5
3	4	B	UPL	88–91	23	210	AF	1	287.0	31.0	16.3	23.2	307.6	15.6	8.1
1	4	U	PL	88–91	11	663	AF	1	274.0	36.0	12.3	14.4	317.4	11.5	6.1

Sources: 1 Clube et al. (1985); 2 Clube and Robertson (1986); 3 Morris et al. (1990); 4 Abrahamsen and Schönharting (1987); 5 McLeod et al. (1990); 6 Allerton and Vine (1990); 7 Bonhommet et al. (1988); 8 Hurst et al. (1992); 9 Varga et al. (1999); 10 Morris et al. (1998); 11 Allerton (1989). *Lithologies:* Sheeted dikes; Upper/Lower Pillow Lavas; Basal Group. *Demagnetisation*: Alternating field, thermal, 1 = pilot study, M = all specimens demagnetised. *Quality criteria*: V = van der Voo (1993) (7 = best) and S = Scalera et al. (1996) (A = best).

magnetizations and the relative temporal relationships of their thermochemical and deformation-modified remanences are unknown, so that the rotation-rate is not yet known. It is also not clear to what degree this rotation overlaps with that of the Troodos microplate.

6. Tectonic interpretation and conclusions

In the Akamas mantle-sequence, both magnetic fabrics and paleomagnetic vectors correlate well with the Troodos mantle-sequence. The mineral orientation-distributions due to AMS reveal an easterly-dipping foliation with a N–S mineral lineation in both terranes, mainly representing an alignment of mafic silicates. This is compatible with mantle-flow up and away from the spreading axes that were located east of Mt. Olympus and which are now oriented N–S. AARM fabrics isolate the orientation-distribution of late-crystallizing oxides. Their foliation is similarly oriented in both areas but the mineral lineation plunges easterly, compatible with flow up and away from the spreading axes. The similarity of primary, AMS fabric orientations in the Akamas and Troodos mantle sequence are too great to be coincidental and it appears that they may be considered as a single structural unit from petrofabrics.

For Akamas and Troodos mantle-sequence rocks, characteristic paleomagnetic vectors are present as B-components (secondary) and A-components (primary). Both yield paleopoles not far removed from the present magnetic pole. These favour magnetization ages younger than ~15 Ma. Although the Akamas A- and B-component magnetizations, and the Troodos B-component magnetizations, were acquired under reversed polarity, there were dozens of Late Tertiary polarity switches (Ogg, 1995; Fig. 11), providing ample opportunity for both mantle-sequences to magnetize, presumably at different times, during exhumation of the Troodos complex (Robertson, 1977). However, rock magnetism reveals some differences

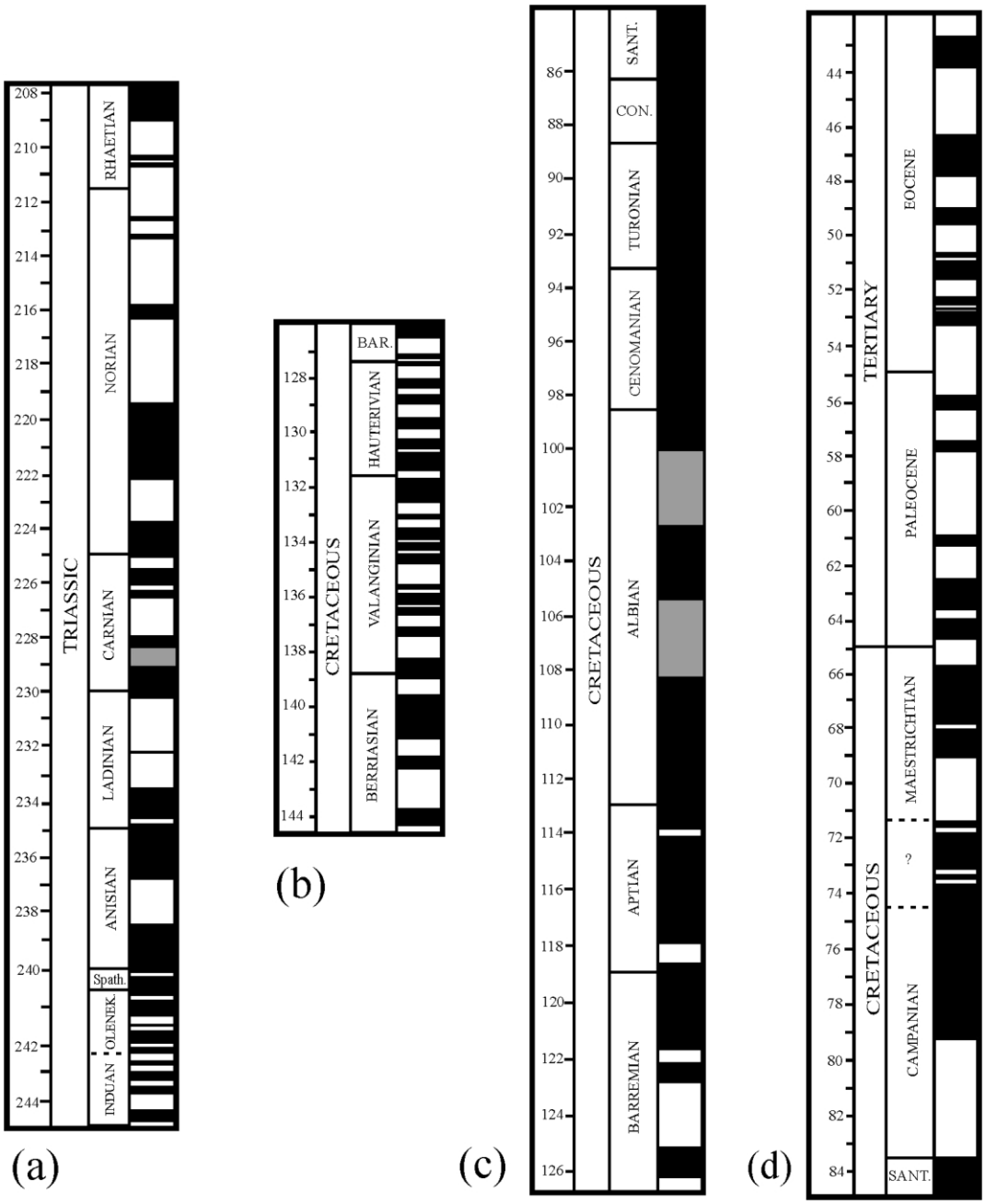

Fig. 11. Magnetostratigraphy for the Triassic to Eocene (Ogg, 1995), (a)–(d), relevant for the respective intervals in which the Triassic Mamonia and Cretaceous Troodos terranes formed.

between the Troodos and Akamas mantle-sequences. In the main Troodos harzburgites, magnetite is almost exclusively responsible for the paleomagnetic signals, hematite being a relatively uninfluential remanence-contributor in the idding-site alteration after olivine. However, the mantle-sequence at Akamas reveals the presence of titanomagnetite characteristic of sea-floor metamorphism, including TM_{60} and titanomaghemite. This may support the view that the Akamas ophiolite is further west of the spreading axis than the main Troodos ophiolite, having had more time and opportunity to undergo hydrothermal alteration, comparable with higher level parts of the ophiolite stratigraphy. The difference in magnetic mineralogy accounts for the different unblocking temperatures, ~250 °C at Akamas and ~475 °C at Troodos, and explains the similar paleopole locations and 'magnetic ages' despite the fact that the more distal Akamas ophiolite may have been exhumed earlier. Since the remanences are in large part chemical rather than thermal, the blocking temperatures do not simply correspond to crustal-isotherm depths.

Older Troodos paleopole locations have been calculated from the characteristic vectors published in earlier studies of higher levels in the ophiolite stratigraphy, from the sheeted dikes, pillowed lavas and sedimentary cover (Table 1). The

paleopoles fall on a convincing APWP, showing that the anticlockwise rotation of ~60° in the interval ~88– ~ 50 Ma occurred about a vertical rotation axis located within the Troodos microplate (Fig. 12b). This is not evident from the changes in declination of magnetic vectors, as previously assumed, but it is proven here because the APWP remains at a constant colatitude with respect to the Troodos microplate (Fig. 10a and b). The APWP construction shows that the subsequent ~30° rotation since 50 Ma, occurred about a different vertical axis because the paleolatitude also changed from an equatorial position to present-day 34°N. Clearly, the Troodos microplate continued its counterclockwise spin at a slower rate. Of course, it is naive simplification to assume that some single rotation-axis is responsible but, if it were the case, the net rotation could be explained by a hypothetical single-rotation axis located far to the west (Fig. 12d). This would account for both the northward drift of the Troodos microplate and the reduced rate of its final component of anticlockwise rotation.

The Mamonia ophiolite exposures may be remanents of Triassic ocean floor, or fragments of the Cretaceous Troodos complex incorporated into the Mamonia terrane. Whatever their age, the high precision vectors obtained by Morris et al. (1988) record the paleomagnetic position since the rocks were penetratively deformed. The paleopoles we determined from these vectors (Table 3) extend the APWP for the Troodos microplate, along the same locus (Fig. 10c). This may imply that the Mamonia terrane underwent rotations through a net arc of ~90°, but it is not yet possible to determine to how much of this rotation postdates docking with the Troodos microplate. The northern provenance suggested for the Mamonia sedimentary rocks is compatible with Clube and Robertson's model (Fig. 12a–c), in which the northern continent and ophiolite slivers become smeared against the northern and eastern margin of Troodos

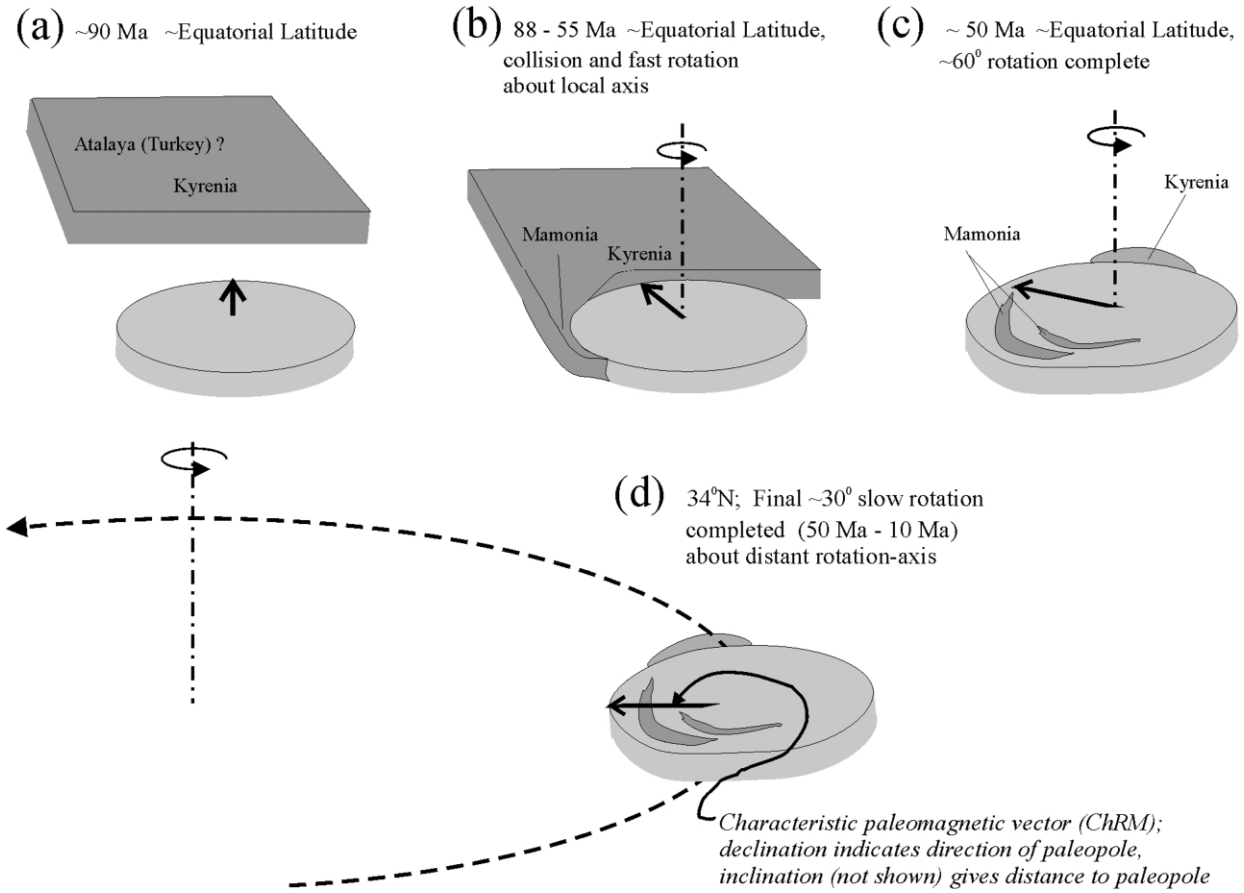

Fig. 12. Plate-tectonic scheme of Clube and Robertson (1986), extended to include the more recent paleomagnetic information and our analysis of it. View is to the north, with the Troodos microplate located above a northward-descending Benioff Zone. (a–c) Early anticlockwise rotation about a local vertical axis within the Troodos microplate (88– ~ 50 Ma), with collision and accretion of Mamonia terrane onto the west and SW margins. Constant equatorial paleolatitude proves that the rotation axis must have been located in or very close to the Troodos microplate (Fig. 10a and b; consider 90° colatitude of paleopoles). Paleopoles within the Mamonia terrane may have been smeared along their APWP (Fig. 10c) due to this internal deformation. (d) Later slower, anticlockwise rotation (post-50 Ma) accompanied by drift from the equator to 34°N, which could be explained geometrically by a single rotation axis, far to the west.

microplate as it spun about its own vertical axis. This may account for the dispersion of Mamonia paleopoles (Fig. 10c) about the same trajectory as those of the Troodos microplate during the early part of the Troodos rotation (Fig. 12a–c). The northward drift due to rotation about some distant vertical-axis is recorded only by young paleopoles in Tertiary sedimentary rocks, and by exhumation-magnetizations of the Troodos–Akamas mantle-sequence. It did not require circum-Troodos tectonic deformation and it is therefore not recorded in the Mamonia APWP.

Acknowledgements

This work was funded by the Natural Sciences and Engineering Research Council of Canada (NSERC) to Graham Borradaile. The work was greatly assisted and encouraged by the Geological Survey Department of Cyprus, in particular through Dr George Petrides (Director) and Dr Ioannis Panayides. Dr Costas Xenophontos provided invaluable logistical support and advice in the early stages of the work. Anne Hammond produced excellent drill core, thin-sections, electron-microscope mounts and mineral separations. David Gauthier is thanked for discussion, for reading the manuscript and especially for help preparing Table 4.

References

Abrahamsen, N., Schönharting, G., 1987. Paleomagnetic timing and translation of Cyprus. Earth and Planetary Science Letters 81, 409–418.

Allerton, S., 1989. Fault block rotations in ophiolites: results of paleomagnetic studies in the Troodos Complex, Cyprus. In: Kissel, C., Laj, C. (Eds.), Paleomagnetic Rotations and Continental Deformation. NATO Conference Volume, Kluwer Academic Press, pp. 393–410.

Allerton, S., Vine, F.J., 1987. Spreading structure of the Troodos ophiolite, Cyprus: some paleomagnetic constraints. Geology 15, 593–597.

Allerton, S., Vine, F.J., 1990. Paleomagnetic and structural studies in the Troodos complex. In: Malpas, J., Moores, E., Panayiotou, A., Xenophontos, C. (Eds.), Proceedings of the Symposium on Ophiolites and Oceanic Lithosphere: TROODOS 87. Geological Survey Department, Nicosia, Cyprus, pp. 99–111.

Bailey, W.R., Holdsworth, R.E., Swarbrick, R.E., 2000. Kinematic history of a reactivated oceanic suture: the Mamonia complex suture zone, SW Cyprus. Journal of the Geological Society, London 157, 1107–1126.

Bonhommet, N., Roperch, P., Calza, F., 1988. Paleomagnetic arguments for block rotations along the Arakapas fault (Cyprus). Geology 16, 422–425.

Borradaile, G.J., 1987. Anisotropy of magnetic susceptibility: rock composition versus strain. Tectonophysics 138, 327–329.

Borradaile, G.J., 1991. Correlation of strain with anisotropy of magnetic susceptibility (AMS). Pure and Applied Geophysics 135, 15–29.

Borradaile, G.J., 1997. Deformation and paleomagnetism. Surveys in Geophysics 18, 405–435.

Borradaile, G.J., 2001a. Magnetic fabrics and petrofabrics: their orientation distributions and anisotropies. Journal of Structural Geology 23, 1581–1596.

Borradaile, G.J., 2001b. Paleomagnetic vectors and tilted dikes. Tectonophysics 333, 417–426.

Borradaile, G.J., 2003. Earth Science Data: Distributions in Frequency, Space, Time and Orientation, Springer-Verlag, Heidelberg, 220pp.

Borradaile, G.J., Dehls, J.F., 1993. Regional kinematics inferred from magnetic subfabrics in Archean rocks of Northern Ontario, Canada. Journal of Structural Geology 15, 887–894.

Borradaile, G.J., Gauthier, D., 2001. AMS-detection of inverse fabrics without AARM, in ophiolite dikes. Geophysical Research Letters 28, 3517–3520.

Borradaile, G.J., Gauthier, D., 2003. Interpreting anomalous magnetic fabrics in ophiolite dikes. Journal of Structural Geology 25, 171–182.

Borradaile, G.J., Henry, B., 1997. Tectonic applications of magnetic susceptibility and its anisotropy. Earth Science Reviews 42, 49–93.

Borradaile, G.J., Lagroix, F., 2001. Magnetic fabrics reveal Upper Mantle Flow fabrics in the Troodos Ophiolite Complex, Cyprus. Journal of Structural Geology 23, 1299–1317.

Borradaile, G.J., Stupavsky, M., 1995. Anisotropy of magnetic susceptibility: measurement schemes. Geophysical Research Letters 22, 1957–1960.

Borradaile, G.J., Werner, T., 1994. Magnetic anisotropy of some phyllosilicates. Tectonophysics 235, 233–248.

Borradaile, G.J., Lagroix, F., Trimble, D., 2001. Improved isolation of archeomagnetic signals by combined low temperature and alternating field demagnetization. Geophysical Journal International 147, 176–182.

Borradaile, G.J., Lucas, K., Middleton, R.S., 2003. Effectiveness of low-temperature demagnetization in the isolation of characteristic remanence. Geophysical Journal International in press.

Clube, T.M.M., Creer, K.M., Robertson, A.H.F., 1985. Palaeorotation of the Troodos microplate, Cyprus. Nature 317, 522–524.

Clube, T.M.M., Robertson, A.H.F., 1986. The palaeorotation of the Troodos microplate, Cyprus, in the Late Mesozoic–Early Cenozoic plate tectonic framework of the Eastern Mediterranean. Surveys in Geophysics 8, 375–437.

Daly, L., Zinsser, H., 1973. Étude comparative des anisotropies de susceptibilité et d'aimantation rémanente isotherme: conséquences pour l'analyse structurale et le paléomagnétisme. Annales Géophysicae 29, 189–200.

Dunlop, D., Özdemir, Ö., 1997. Rock Magnetism: Fundamentals and Frontiers, Cambridge University Press, 573pp.

Ealy, P.J., Knox, G.J., 1975. The pre-Tertiary rocks of SW Cyprus. Contributions to Mineralogy and Petrology 89, 239–255.

Flinn, D., 1962. On folding during three-dimensional progressive deformation. Geological Society of London, Quarterly Journal 118, 385–428.

Flinn, D., 1965. On the symmetry principle and the deformation ellipsoid. Geological Magazine 102, 36–45.

Gass, I.G., 1968. Is the Troodos massif of Cyprus a fragment of Mesozoic Ocean floor? Nature 221, 926–930.

Gass, I.G., MacLeod, C.J., Murton, B.J., Panayiotou, A., Siimonian, K.O., Xenophontos, C., 1994. The Geology of the Southern Troodos Transform Fault Zone. Memoir 9, Geological Survey Department, Ministry of Agriculture, Nicosia, Cyprus, 218pp.

Gee, J.S., Varga, R.J., Gallet, P., Staudigel, H., 1993. Reversed-polarity overprint in dikes from the Troodos ophiolite: implications for the timing of alteration and extension. Geology 21, 849–852.

Henson, F.R.S., Browne, R.V., McGinty, J., 1949. A synopsis of the stratigraphy and geological history of Cyprus. Geological Society of London, Quarterly Journal 105, 1–41.

Hrouda, F., 1982. Magnetic anisotropy of rocks and its application in geology and geophysics, Geophysical Surveys 5, 37–82.

Hurst, S.D., Verosub, K.L., Moores, E.M., 1992. Paleomagnetic constraints on the formation of the Solea graben, Troodos ophiolite, Cyprus. Tectonophysics 208, 431–445.

Jackson, M.J., 1991. Anisotropy of magnetic remanence: a brief review of mineralogical sources, physical origins, and geological applications, and comparison with susceptibility anisotropy. Pure and Applied Geophysics 136, 1–28.

Jackson, M.J., Sprowl, D., Ellwood, B., 1989. Anisotropies of partial anhysteretic remanence and susceptibility in compacted black shales: grain-size and composition-dependent magnetic fabric. Geophysical Research Letters 16, 1063–1066.

Jelinek, V., 1977. The Statistical Theory of Measuring Anisotropy of Magnetic Susceptibility of Rocks and its Application, Geofyzika, Brno, 88pp.

Jelinek, V., 1978. Statistical processing of anisotropy of magnetic susceptibility measured on groups of specimens. Studia Geophica et Geodetica 22, 50–62.

Jelinek, V., 1981. Characterization of the magnetic fabrics of rocks. Tectonophysics 79, T63–T67.

Jelinek, V., 1985. The physical principles of measuring magnetic anisotropy with the torque magnetometer. Travaux Geophysiques 33, 177–198.

Jelinek, V., 1996. Theory and measurement of the anisotropy of isothermal remanent magnetization of rocks. Travaux Géophysiques 37, 124–134.

Kirschvink, J.L., 1980. The least squares line and plane and the analysis of paleomagnetic data. Geophysical Journal of the Royal Astronomical Society 62, 699–718.

Lagroix, F., Borradaile, G.J., 2000. Magnetic fabric interpretation complicated by inclusions in mafic silicates. Tectonophysics 325, 207–225.

Lagroix, F., Borradaile, G.J., 2001. Tectonics of the circum-Troodos sedimentary cover of Cyprus, from rock magnetic and structural observations. Journal of Structural Geology 22, 453–469.

LaPierre, H., Rocci, G., 1969. Un bel exemple d'association cogénetique laves-radiolarites-calcaires: la formation Triassique de Petra tou Romiou (Chypre). C.R. Acad. Sci. Paris, Ser. D 268, 2637–2640.

MacDonald, W.D., 1980. Net tectonic rotation, apparent tectonic rotation, and the structural tilt correction in paleomagnetic studies. Journal of Geophysical Research 85, 3659–3669.

MacLeod, C.J., Allerton, S., Gass, I.G., Xenophontos, C., 1990. Structure of a fossil ridge-transform intersection in the Troodos ophiolite. Nature 348, 717–720.

Malpas, J., Moores, E., Panayiotou, A., Xenophontos, C. (Eds.), 1990. Ophiolites: Oceanic Crustal Analogues ("Troodos 1987" Conference Volume). Cyprus Geological Survey Department, Nicosia, Cyprus, 733pp.

Malpas, J., Calon, T., Squires, G., 1993. The development of a late Cretaceous microplate suture zone in SW Cyprus. In: Prichard, H.M., Alabaster, T., Harris, N.B., Neary, C.R. (Eds.), Magmatic Processes and Plate Tectonics. Geological Society of London, Special Publication 76, pp. 177–195.

McCabe, C., Jackson, M.J., Ellwood, B.B., 1985. Magnetic anisotropy in the Trenton limestone: results of a new technique, anisotropy of anhysteretic susceptibility. Geophysical Research Letters 12, 333–336.

Moores, E.M., Vine, F.J., 1971. The Troodos Massif, Cyprus and other ophiolites as oceanic crust: evaluation, implications. Philosophical Transactions of the Royal Society of London, Series A 268, 443–466.

Moores, E.M., Varga, R.J., Verosub, K.L., Ramsden, T., 1990. Regional structure of the Troodos Dike Complex. In: Malpas, J., Moores, E.M., Panayioutou, A., Xenophontos, C. (Eds.), Ophiolites. Oceanic crustal Analogues ("Troodos 1987" Conference Volume). Cyprus Geological Survey Department, Nicosia, Cyprus, pp. 53–64.

Moores, E.M., Kellogg, L.H., Dilek, Y., 2000. Tethyan ophiolites, mantle convection, and tectonic "historical contingency": a resolution of the "ophiolite conundrum". In: Dilek, Y., Moores, E.M., Elthon, D., Nicolas, A. (Eds.), Ophiolites and Oceanic Crust: New Insights from Field Studies and the Ocean Drilling Program. Geological Society of America, Special Paper 349, pp. 3–12.

Morris, A., 1996. A review of paleomagnetic research in the Troodos ophiolite, Cyprus. In: Morris, A., Tarling, D.H. (Eds.), Paleomagnetism and Tectonics of the Mediterranean Region. Geological Society of London, Special Publication 105, pp. 311–324.

Morris, A., Creer, K.M., Robertson, A.H.F., 1990. Paleomagnetic evidence for clockwise rotations related to dextral shear along the Southern Troodos Transform Fault (Cyprus). Earth and Planetary Science Letters 99, 250–262.

Morris, A., Anderson, M.W., Robertson, A.H.F., 1998. Multiple tectonic rotations and transform tectonism in an intraoceanic suture zone, SW Cyprus. Tectonophysics 299, 229–253.

Muxworthy, A., Dunlop, D.J., Özdemir, Ö., 2003. Low-temperature cycling of isothermal and anhysteretic remanence: microcoercivity and magnetic memory. Earth and Planetary Science Letters 205, 173–184.

Nakamura, N., Borradaile, G.J., 2001a. Strain, anisotropy of anhysteretic remanence, and anisotropy of magnetic susceptibility in a slaty tuff. Physics of the Earth and Planetary Interiors 125, 85–93.

Nakamura, N., Borradaile, G.J., 2001b. Do reduction spheroids predate finite strain? A magnetic diagnosis of Cambrian slates in North Wales. Tectonophysics 304, 133–139.

Nye, J.F., 1957. Physical Properties of Crystals, Oxford University Press, New York, 329pp.

Ogg, J.G., 1995. Magnetic polarity time-scale for the Phanerozoic. In: Ahrens, T.J. (Ed.), Global Earth Physics: A Handbook of Geophysical Constants. American Geophysical Union, Reference Shelf no. 1, pp. 225–270.

Parma, J., 1988. An automated torque meter for rapid measurement of high-field magnetic anisotropy of rocks. Physics of the Earth and Planetary Interiors 51, 387–389.

Potter, D.K., Stephenson, A., 1990. Field-impressed magnetic anisotropy in rocks. Geophysical Research Letters 17, 2437–2440.

Robertson, A.H.F., 1977. Tertiary uplift history of the Troodos massif, Cyprus. Geological Society of America Bulletin 88, 1763–1772.

Robertson, A.H.F., 1990. Tectonic evolution of Cyprus. In: Malpas, J., Moores, E.M., Panayioutou, A., Xenophontos, C. (Eds.), Ophiolites: Oceanic Crustal Analogues ("Troodos 1987" Conference Volume). Cyprus Geological Survey Department, Nicosia, Cyprus, pp. 235–250.

Robertson, A.H.F., Woodcock, N.H., 1979. The Mamonia Complex, south-west Cyprus: the evolution and emplacement of a Mesozoic continental margin, Geological Society of America Bulletin 90, 651–665.

Robertson, A.H.F., Xenophontos, C., 1993. Development of concepts concerning the Troodos ophiolite and adjacent units in Cyprus. In: H.M. Prichard, T. Alabaster. T. Harris (eds.) Magmatic Processes and Plate Tectonics. Special Publication of the Geological Society of London, 70, 85–120.

Rochette, P., Jenatton, L., Dupuy, C., Boudier, F., Reuber, I., 1991. Emplacement modes of basaltic dykes in the Oman ophiolite: evidence from magnetic anisotropy with reference to geochemical studies. In: Peters, Tj., (Ed.), Ophiolite Genesis and the Evolution of the Oceanic Lithosphere. Ministry of Petroleum and Minerals, Sultanate of Oman, Kluwer, Dordrecht, pp. 55–82.

Rochette, P., Jackson, J., Aubourg, C., 1992. Rock magnetism and the interpretation of anisotropy of magnetic susceptibility. Reviews of Geophys 30, 209–226.

Rochette, P., Aubourg, C., Perrin, M., 1999. Is this magnetic fabric normal? A review and case studies in volcanic formations. Tectonophysics 307, 219–234.

Scalera, G., Favali, P., Florindo, F., 1996. Paleomagnetic database: the effect of quality filtering for geodynamic studies. In Morris, A., Tarling, D.H. (Eds.), Paleomagnetism and Tectonics of the Mediterranean Region. Geological Society of London, Special Publication 105, pp. 225–237.

Stacey, F.D., Banerjee, S.K., 1967. The highfield torquemeter method of measuring magnetic anisotropy in rocks. In: Collinson, D.W., Creer, K.M., Runcorn, S.K. (Eds.), Methods in Paleomagnetism, Elsevier, New York, pp. 470–476.

Stephenson, A., Potter, D.K., 1996. Towards a quantitative description of field-impressed anisotropy of susceptibility. Geophysical Journal International 126, 505–512.

Stephenson, A., Sadikun, S., Potter, D.K., 1986. A theoretical and experimental comparison of the anisotropies of magnetic susceptibility and remanence in rocks and minerals. Geophysical Journal of the Royal Astronomical Society 84, 185–200.

Swarbrick, R.E., 1993. Sinistral strike-slip and tranpressional tectonics in an ancient ocean setting: the Mamonia Complex. South-west Cyprus, Journal of the Geological Society of London 150, 381–392.

van der Voo, R., 1993. Paleomagnetism of the Atlantic, Tethys and Iapetus Oceans, Cambridge University Press, Cambridge, 411pp.

Varga, R.J., Moores, E.M., 1985. Spreading structure of the Troodos ophiolite, Cyprus. Geology 13, 846–850.

Varga, R.J., Gee, J.S., Bettison-Varga, L., Anderson, R.S., Johnson, C.L., 1999. Early establishment of seafloor hydrothermal systems during structural extension: paleomagnetic evidence from the Troodos ophiolite, Cyprus. Earth and Planetary Science Letters 171, 221–235.

Vine, F.J., 1966. Spreading of the ocean-floor: new evidence. Science 154, 1405–1415.

Vine, F.J., Matthews, D.H., 1963. Magnetic anomalies over ocean-ridges. Nature 199, 947–949.

Vine, F.J., Moores, E.M., 1969. Paleomagnetic results from the Troodos igneous massif, Cyprus. Transactions of the American Geophysical Union 50, 131.

Whitechurch, H., Juteau, T., Montigny, R., 1986. Role of the Eastern Mediterranean ophiolites (Turkey, Syria, Cyprus) in the history of Neo-Tethys. In: Dixon, J.E., Roberston, A.H.F. (Eds.), Geological Evolution of the Eastern Mediterranean. Geological Society of London, Special Publication 17, pp. 301–317.

Woodcock, N.H., 1977. Specification of fabric shapes using an Eigenvalue method. Geological Society of America Bulletin 88, 1231–1236.

Zijderveld, J.D.A., 1967. AC demagnetization of rocks: analysis of results. In: Collinson, D.W., Creer, K.M., Runcorn, S.K. (Eds.), Methods in Paleomagnetism, Elsevier, New York, pp. 254–256.